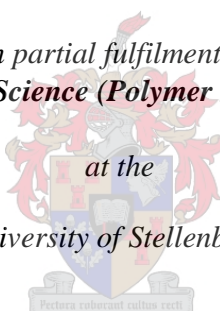# The scaling up of highly filled polymer clay nanocomposites with regard to clay loading

by

Kerissa Moodley

Thesis presented in partial fulfilment of the degree of
Master of Science (Polymer Science)

at the

University of Stellenbosch

Supervisor: Professor. Harald Pasch

December 2016

Declaration

By submitting this thesis electronically, I declare that the entirety of the work contained therein is my own, original work, that I am the sole author thereof (save to the extent explicitly otherwise stated), that reproduction and publication thereof by Stellenbosch University will not infringe any third party rights and that I have not previously in its entirety or in part submitted it for obtaining any qualification.

K. Moodley   December 2016

Abstract

Water-based polymer clay nanocomposites (PCN) based on styrene-co-butyl acrylate copolymers (PSBA/MMT) were prepared with clay loadings of up to 50 wt.%. The resultant materials showed instability with regard to particle size and morphology due to increased viscosity of the dispersion which was further evidenced by transmission electron microscopy (TEM) and dynamic light scattering (DLS). Additionally the dry films were found to show exfoliated to intercalated clay platelet morphologies in the polymer matrix as the amount of clay increased. These latexes showed increasing glass transition temperatures (T_g) with clay loadings up to 40 wt.%, which was attributed to the clay platelets absorbing the heat. Increasing the loading to 50 wt.% showed a decrease in T_g which was due to restricted molecular motions of the polymer in the nanocomposite. Thermal stability, determined using TGA, showed a decreasing trend as the amount of clay present in the PCNs increased.

The next part of the study was dedicated to scaling up the current procedure to suit industrial needs and thus the PCNs were prepared without the use of typical emulsification devices. The hybrid latexes obtained showed unstable particles as well as large amounts of coagulum as the amount of clay present in the latexes increased. Dynamic mechanical analysis (DMA) results were contradictory to those of the latexes produced on a smaller scale. This was due to melt pressing of the films which caused crosslinking of the polymer and exhibited an increasing storage modulus as the clay loading increased. The T_gs showed similar results to those of the PSBA/MMT latexes. The thermal stability of the films showed a similar onset peak with the exception of the 50 wt.% sample which showed a higher onset temperature. This is confirmed with the use of TEM which shows heterogeneous dispersion of clay platelets which could lead to the early onset temperature. The overall stability of the latexes decreased as the amount of clay present in the PCN's increased and using a clay content of 50 wt.% is unsuitable.

The comparison of these scaled up nanocomposites to the ones prepared on the lab scale shows that the material properties are compromised.

Opsomming

Water-gebaseerde polimeer klei nanosamestellings (PKN) gebaseer op stireen-mede-butylacrylaat kopolimere (PSBA / MMT) bereid was om met 'n hoë klei beladings van tot 50 wt.%. Die gevolglike materiaal gewys onstabiliteit met betrekking tot deeltjiegrootte en morfologie as gevolg van verhoogde viskositeit van die verstrooiing wat verder bewys deur transmissie elektronmikroskopie (TEM) en dinamiese lig verstrooiing (DLS). Verder die droë films gevind om te wys exfoliated om interkalêre klei plaatjie morfologieen in die polimeermatriks as die bedrag van klei toegeneem. Hierdie latexes getoon toenemende glasoorgangstemperature (T_g) met klei beladings tot 40 wt.%, Wat toegeskryf word aan die klei plaatjies absorbeer die hitte. Die verhoging van die laai tot 50 wt.% toon 'n afname in T_g wat as gevolg van beperkte molekulêre bewegings van die polimeer in die nanosaamgestelde was. Termiese stabiliteit, bepaal met behulp van TGA, het 'n dalende neiging as die bedrag van klei teenwoordig in die PKNs toegeneem.

Die volgende deel van die studie is gewy aan verhoogde gebruik die huidige prosedure wat gevolg moet industriële behoeftes en dus is die PKNs voorberei sonder die gebruik van tipiese emulsifisering toestelle te pas. Die baster latexes verkry het onstabiele deeltjies asook groot hoeveelhede coagulum as die bedrag van klei teenwoordig is in die latexes toegeneem. Dinamiese meganiese analise (DMA) resultate was teenstrydig met dié van die latexes geproduseer op 'n kleiner skaal. Dit was as gevolg van smelt druk van die films wat kruisbinding van die polimeer veroorsaak en uitgestal 'n toenemende stoor modulus soos klei laai toegeneem. Die T_g se gewys soortgelyke resultate met dié van die PSBA / MMT latexes. Die termiese stabiliteit van die films het 'n soortgelyke aanvang hoogtepunt met die uitsondering van die 50 wt.% monster wat 'n hoër aanvang temperatuur gewys. Dit word bevestig met die gebruik van TEM wat skeef verspreiding van klei plaatjies wat kan lei tot die vroeë aanvang temperatuur toon. Die algehele stabiliteit van die latexes afgeneem as die bedrag van klei teenwoordig is in die PKN se verhoogde en met behulp van 'n klei-inhoud van 50 wt.% ongeskik is.

Die vergelyking van hierdie afgeskaal tot nanosamestellings die kinders voorberei op die laboratorium skaal dui daarop dat die materiaal eienskappe gekompromitteer.

Acknowledgements

Contents

List of Figures

List Tables

List of abbreviations

PSBA	poly(styrene-co-butyl acrylate)
MMT	montmorillonite clay
VBDAC	vinylbenzyldodecyldimethylammonium chloride
PSBA-MMT	poly(styrene-co-butyl acrylate)/montmorillonite nanocomposite
MMT-VBDA	montmorillonite modified with vinylbenzyldodecyldimethylammonium chloride
PCN	polymer-clay nanocomposite
AIBN	azobisisobutyronitrile
SDS	sodium dodecyl sulphate
HD	hexadecane
MEHQ	mono methyl ether hydroquinone
KOH	potassium hydroxide
THF	tetrahydrofuran
T_g	glass transition temperature
T_{onset}	onset temperature of decomposition
CEC	cation exchange capacity
NMR	nuclear magnetic resonance
FTIR	fourier transform infrared spectroscopy
TEM	transmission electron microscopy
DSC	differential scanning calorimetry
DMA	dynamic mechanical analysis
TGA	thermogravimetric analysis

1   Introduction and objectives

1.1   Introduction:

Research in nanotechnology has expanded exponentially in the last decade, making it an ideal area for development of tailor-made materials[1–8]. Commercially, this is appealing due to the need for alternative resources which provide economically and environmentally friendly options. Polymer-clay nanocomposites (PCNs) have broadened the field of application for synthetic polymer materials. The polymer matrix is reinforced with an inorganic filler (clay in this case) which results in enhanced thermal, mechanical, barrier and optical properties[1,3,4,6,7,9–13]. There are numerous reports of these inorganic inclusions incorporated at a low weight percentage relative to the polymer (less than 10%)[10,11,14–19]resulting in increased material properties. Very few studies related to large amounts of inorganic filler incorporated into polymers are found in literature. This type of polymer nanocomposite is of relevance commercially since it provides an economically viable route to new materials that are reinforced in comparison to the pristine polymer. Clays are found in natural abundance and thus are relatively low cost compounds. This has made it an attractive option to be combined with polymers in terms of decreasing cost if large amounts of clay are incorporated into these materials.

Polymer nanocomposites may have different morphologies and their inorganic components reflect what applications they may be suitable to.

Producing these nanocomposites on a lab scale includes the use of a complex miniemulsion procedure. However the reaction setup differs in an industrial environment where larger volumes are synthesised and the process needs to be within financial limits. Thus, the need arises for the adaptation of the lab scale procedure to a manufacturing one.

The work discussed in this thesis tackles the challenges of incorporating large amounts of clay into a polymer matrix as well as creating an applicable process that is commercially feasible. Additionally the physical properties of these materials are investigated in order to determine whether these materials are superior to the neat polymers.

1.2   Goals and objectives:

The main objective of the project is to prepare polymer-clay nanocomposites (PCNs) on a large scale using an inexpensive nanofiller material. The synthesised PCNs shall be used for coating applications.

The main aims of the project are to:

1. Synthesize water-based styrene-co-butyl acrylate copolymers (PSBA/MMT) latexes:

   - Synthesise the neat polymer and investigate the molar mass and chemical composition

   - Synthesise PCNs with different amounts of clay loadings up to 50wt.%.

   - Investigate the morphology of the nanocomposites

   - Investigate the thermal stability and thermomechanical properties of the nanocomposites

2. Scaling up of the preparation (PSBA/MMT latexes) method

   - Investigate the morphology of the nanocomposites

   - Synthesise PCNs with different amounts of clay loadings up to 50wt.%.
   - Investigate the thermal stability and thermomechanical properties of the nanocomposites

1.3   Thesis layout:

The thesis is composed of an introductory part along with objectives in Chapter 1.

Chapter 2 covers the field of PCNs from preparation to analysis as well as an account of miniemulsion and how it can be translated industrially. Special reference is given to clay fillers as the inorganic component of the PCNs.

In Chapter 3 the latexes are produced using a lab scale preparation of poly (styrene-co-butyl acrylate) /montmorillonite clay (PSBA-MMT) latexes and films with varying MMT contents of up to 50 wt.%, via the miniemulsion polymerization method are described. The characterization methods of the latexes and films are also given.

The processing of the PCN's as in Chapter 3 are discussed using a scaled up method in Chapter 4.

The final conclusions and summary of the work with future recommendations presented are stated in Chapter 5.

1.4   References

1.   Etmimi, H. M. PhD,Stellenbosch, **2012**.

2.   Thostenson, E. T.; Li, C.; Chou, T. *Compos. Sci. Technol.* **2005**, 65, 491–516.

3.   Ray, S. S.; Okamoto, M. *Prog. Polym. Sci.* **2003,** 28**,** 1539–1641.

4.   Jordan, J.; Jacob, K. I.; Tannenbaum, R.;Sharaf, M. A.; Jasiuk, I. *Mater. Sci. Eng. A–Struct.* **2005**, 393, 1–11.

5.   Qi, D.; Cao, Z.; Ziener, U. *Adv. Colloid Interface Sci.* **2014***,* 211, 47–62.

6.   Schmidt, G.; Malwitz, M. M. *Curr. Opin. Colloid Interface Sci.* **2003**, 8, 103–108.

7.   Gao, F. *Mater. Today* **2004**, 7, 50–55.

8.   Bourgeat-lami, E. *Encycl. Nanosci. Nanotechnol.* **2004**, 8, 305–332.

9.   García-Chávez, K. I.; Hernández-Escobar, C. A.; Flores-Gallardo, S. G.; Soriano Corral, F.; Saucedo-Salazar, E.; Zaragoza-Contreras, E. A. *Micron,* **2013**, 49, 21–27.

10.   Tsai, T.; Lin, M.; Chang, C.; Li, C. *J. Phys. Chem. Solids* **2010**, 71, 590–594.

11.   Bouanani, F.; Bendedouch, D.; Hemery, P.; Bounaceur, B. *Colloids Surfaces A Physicochem. Eng. Asp.* **2008**, 317, 751.

12.   Hybrid Latex Particles, ed. E. Bourgeat-Lami; M. Lansalot, **2009**, 53-124.

13.   Zengeni, E.; Hartmann, P. C.; Pasch, H. *Compos. Sci. Technol.* **2013**, 84**,** 31–38.

14.   Voorn, D. J.; Ming, W.; Van Herk, A. M. *Macromol.* **2006**, 39, 4654–4656.

15.   Alshabanat, M.; Al-Arrash, A.; Mekhamer, W. J. *Nanomater.* **2013,** 2013, Article ID 650725.

16.   Voorn, D. J.; Ming, W.; Herk, A. M.; Van Bomans, P. H. H.; Frederik, P. M.; Gasemjit, P.; Johanssmann, D. *Langmuir.* **2005**, 21, 6950–6956.

17.   Utracki, L. A. *IEEE Electr. Insul. Mag.* **2010**, 26, 6–15.

18.   Asua, M.; Paulis, M.; Leiza, J. R.; Diaconu, G. *Macromol. Symp.* **2007,** 259, 305–317.

19.   Ka, F.; Fekete, E. *Langmuir* **2006**, 22, 7848–785

2   Literature review

2.1   Nanocomposites

Composites have been developed out of a need for materials that exhibit a specific combination of enhanced thermal, barrier and optical properties, to mention a few, that a single type of material cannot provide. They typically consist of an organic and an inorganic component with the latter's dimensions in the order of nanometres. Nanocomposites possess fine dimensions on the order of nanometres which are similar to those of polymers. Types of reinforcing material added include nanofibres[1–3](carbon nanotubes), nanoparticles (carbon black[4], metal[1,5] and silica[6]) and nanoplatelets (graphene[1] and clay [3,7,8]). All of these materials offer improved properties due to the high aspect ratio of the inorganic component and its interaction with the polymer [2,4]. The area of polymer clay nanocomposites (PCNs) is of particular interest in both industry and the academic world. This is due to the enhanced thermomechanical [9–13], optical[3,14–18], barrier[19–21] properties and chemical resistance[10,17,22], to name a few, of the hybrid materials in comparison to the neat polymer.

2.1.1   *Polymer clay nanocomposites:*

PCN's are hybrid nanomaterials which conventionally have a relatively low weight percentage, typically 1-5 wt.%, of clay platelets embedded into a polymer matrix. Clay consists of stacks of platelets called tactoids and the dimensions of these tactoids are in the order of nanometres[11,13,22,23]. During synthesis, polymer chains can enter the spaces between the platelets, known as galleries or interlayer spaces, thus incorporating the clay into the polymer matrix. The resulting materials form different morphologies depending on factors such as dispersion and compatibility of the clay, with regard to the polymer which are discussed below:

- Conventional composites

They are composed of stacks of clay tactoids and are also referred to as microcomposites. Since the interlayer space has not expanded, the polymer chains do not penetrate the galleries of the tactoids. This produces a heterogeneous composite as seen in Figure 2.1(a) (microphase separation) which shows hardly any improved properties.

- Intercalated nanocomposites:

The gallery spacing increases but still remains primarily oriented in the stacks of tactoids as illustrated in Figure 2.1(b). However the polymer is able to penetrate the galleries. There is an improvement in the thermal and mechanical properties compared to the neat polymer.

- Exfoliated nanocomposites

The individual silicate sheets are fully separated and do not interact with each other and are thus randomly orientated as shown in Figure 2.1(c). They are usually homogenously distributed throughout the polymer matrix and thus yield the most enhanced properties relative to the bulk polymer.
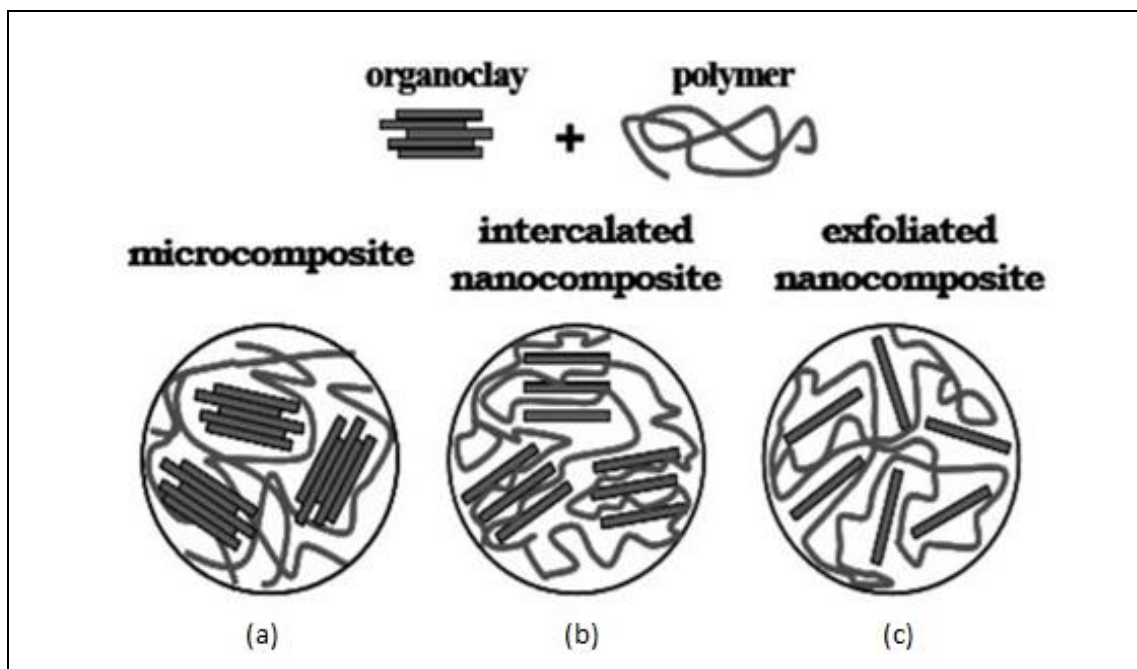
Figure 2.1: Different structures of polymer clay nanocomposites (a) microcomposite, (b) intercalated nanocomposite, (c) exfoliated nanocomposite[10]

2.2   Clay as an inorganic filler

With the vast amount of research done on the topic of PCN's the choice of clay selected has been those in the phyllosilicate class. The clay structure in this group is made up of layered sheets stacked together which are hydrophilic in nature. The natural abundance of these minerals make them a viable inexpensive material[24]. The phyllosilicate class can be further subdivided into two categories, that being: 1:1 non-swelling clays such as Kaolin and 2:1

swelling clays such as Laponite and Montmorillonite (MMT). There are different classes and types of clays available ranging from natural clays such as kaolin and to synthetic clays such as Laponite. These layered silicates can be further subdivided regarding their chemical structure and composition i.e. smectite clays, such as MMT, which are swellable and kaolinites, such as kaolin, which are not swellable[24].

MMT is of particular interest due to its natural abundance, its dimensions (illustrated in Figure 2.2(a)) and high aspect ratio[16,24,25]. Figure 2.2 (b)[11] shows that the structure of these layered silicates contains two silica tetrahedral sheets that sandwich an octahedral aluminium or magnesium sheet. These platelets are held together by electrostatic forces and are negatively charged[26]. The interlayer spaces are occupied by either sodium (Na^+) or calcium (Ca^+) cations[25]. This is referred to as pristine Na-MMT (or Ca-MMT), however, in this form the clay may not be compatible with the chosen polymer matrix since it is hydrophilic but by modifying the surface the clay can be made hydrophobic.
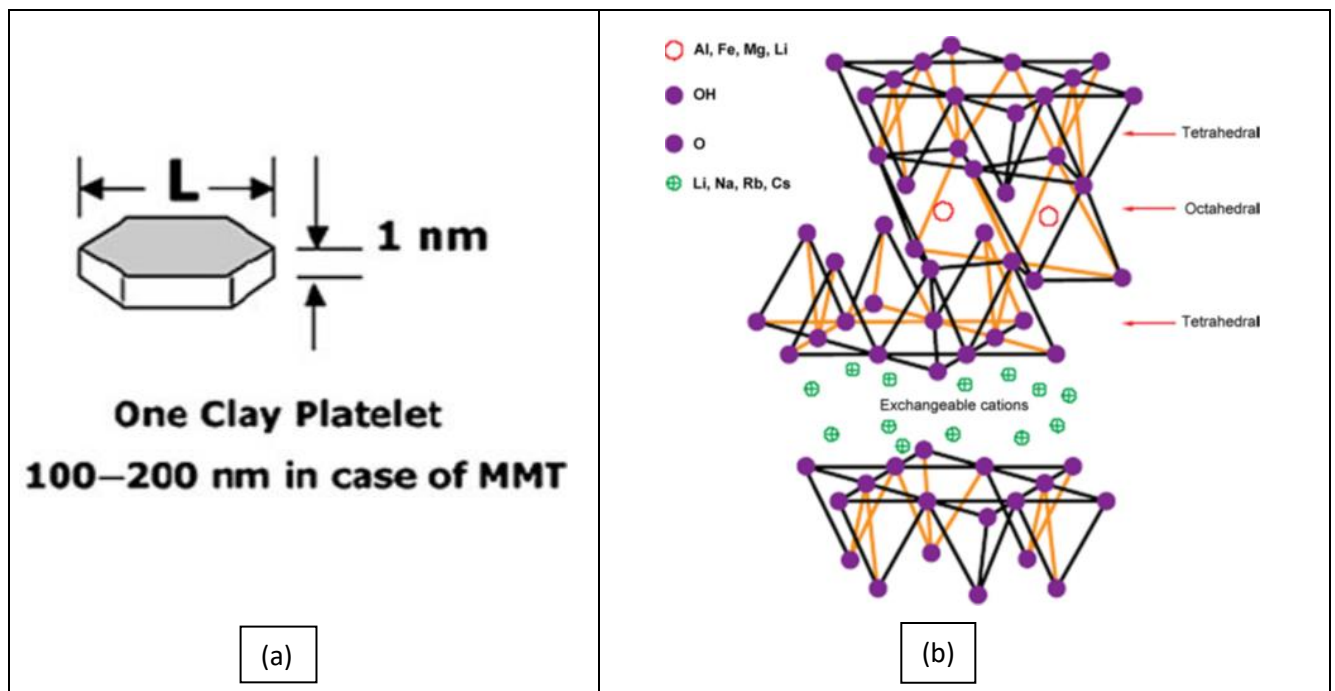
Figure 2.2: (a) Dimensions of MMT and (b) chemical structure of MMT clay

2.3   Clay modification

Pristine Na-MMT is hydrophilic and is not compatible with a hydrophobic polymer matrix. By modifying the surface of the platelets the clay can be made hydrophobic using a surfactant

with the product being referred to as organoclay. As mentioned in Section 2.2 the MMT requires a cationic species to counteract the negative atoms at the platelet surface. This surface charge is referred to as the cationic exchange capacity (CEC). MMT has a high CEC value compared to other clays.

With regard to the surfactants utilized, there is a variety that assists in the delamination process. In particular, quaternary ammonium surfactants[26] are commercially available and contain characteristic alkyl chains in their chemical structure, however, quaternary phosphonium surfactants[14] add an element of increased thermal stability in comparison to the ammonium constituents. These surfactants do not attach strongly to the surface which makes this a drawback since they can be desorbed from the platelets[27]. Additionally, the organic modifiers can be functionalized such that they interact with the monomer as well as separate the platelets and they are referred to as polymerizable surfactants[21,28]. There are different methods by which MMT can be modified as presented throughout literature[11,26,29].

The method of ion exchange in terms of modifying MMT seems to be popular and relatively simple. From Figure 2.3[30] the reaction demonstrates the exchangeable cations i.e. Na^+ being interchanged with surfactants on the surface of the platelets in the form of organic cations[14,21,31] These cations lessen the clays' surface energy and as a result increase the wetting of the monomer and allows them to penetrate into the galleries. This was demonstrated by Singla et al. [26] who successfully treated Na-MMT with a variety of organic cationic surfactants with zinc stearate being the most effective of all the options.
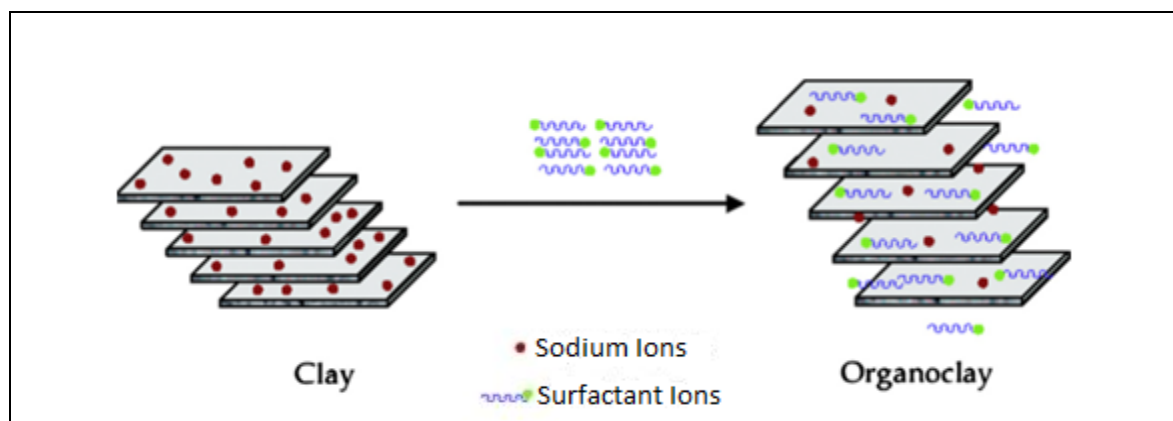
Figure2.3: Ion exchange of clay platelets and surfactant

2.4   Methods of preparation

The various routes to synthesize PCNs have emerged out of a need to properly disperse the clay platelets into the polymer to form a homogenous mixture. The most common techniques, in-situ polymerization[6-8], solution intercalation and melt intercalation[10,11,13], will be discussed below.

2.4.1   Melt intercalation

Melt intercalation is the most industrially relevant and the oldest technique[10,16]. It involves the polymer and the clay mixture being under continuous shear (in an extruder) above the softening point of the polymer. In their molten state the polymer chains diffuse into the galleries of the clay as illustrated in Figure 2.4(a). They can either form exfoliated or intercalated structures depending on the degree of penetration[7]. A wide variety of polymers are compatible with clay using this technique[32]; examples include polyamide 6[11,25], polystyrene and polyethylene oxide (PEO)[33]. An example of this technique is the manufacturing of injection molded polyolefin/clay nanocomposites to form tougher materials. However, this is restricted by the application of materials produced.

2.4.2   Solution intercalation

This technique requires a solvent that is compatible with the polymer as well as causing the clay to swell as shown in Figure 2.4(b). Once the clay is dispersed into the polymer solution the chains of the polymer displace the solvent in the galleries and it is removed by solvent evaporation or polymer precipitation. Chen and Evans[34] used this method to prepare polyethylene glycol (PEG) clay nanocomposites in order to determine whether high molecular mass fractions of polymer intercalate preferentially during polymerization. This helps to explain the reinforcement of intercalated clay particles in the polymer matrix[15,25]. The disadvantages of preparing PCNs in this way is the need to identify compatible pairs of solvent/polymer. Control of the clay dispersion quality[16] is problematic as well as solvent disposal not being environmentally friendly.

2.4.3   In-situ polymerization

In-situ polymerization involves the use of monomer to swell the clay with polymerization taking place between the galleries and in doing so expanding the interlayer space causing further dispersion of the platelets as shown in Figure 2.4(c) [6,25]. Perhaps the most widely known example of this process is that of the Toyota research group which synthesized nylon 6/MMT nanocomposites with dramatically improved properties[25]. Unlike the previous techniques mentioned this one provides control over the dispersion and manipulation of the

final material with complex structures that can be applied in different types of polymerization processes. Of particular interest is heterogeneous polymerization due to its positive environmental influence as well as complete dispersion of organophilic MMT with the use of water.
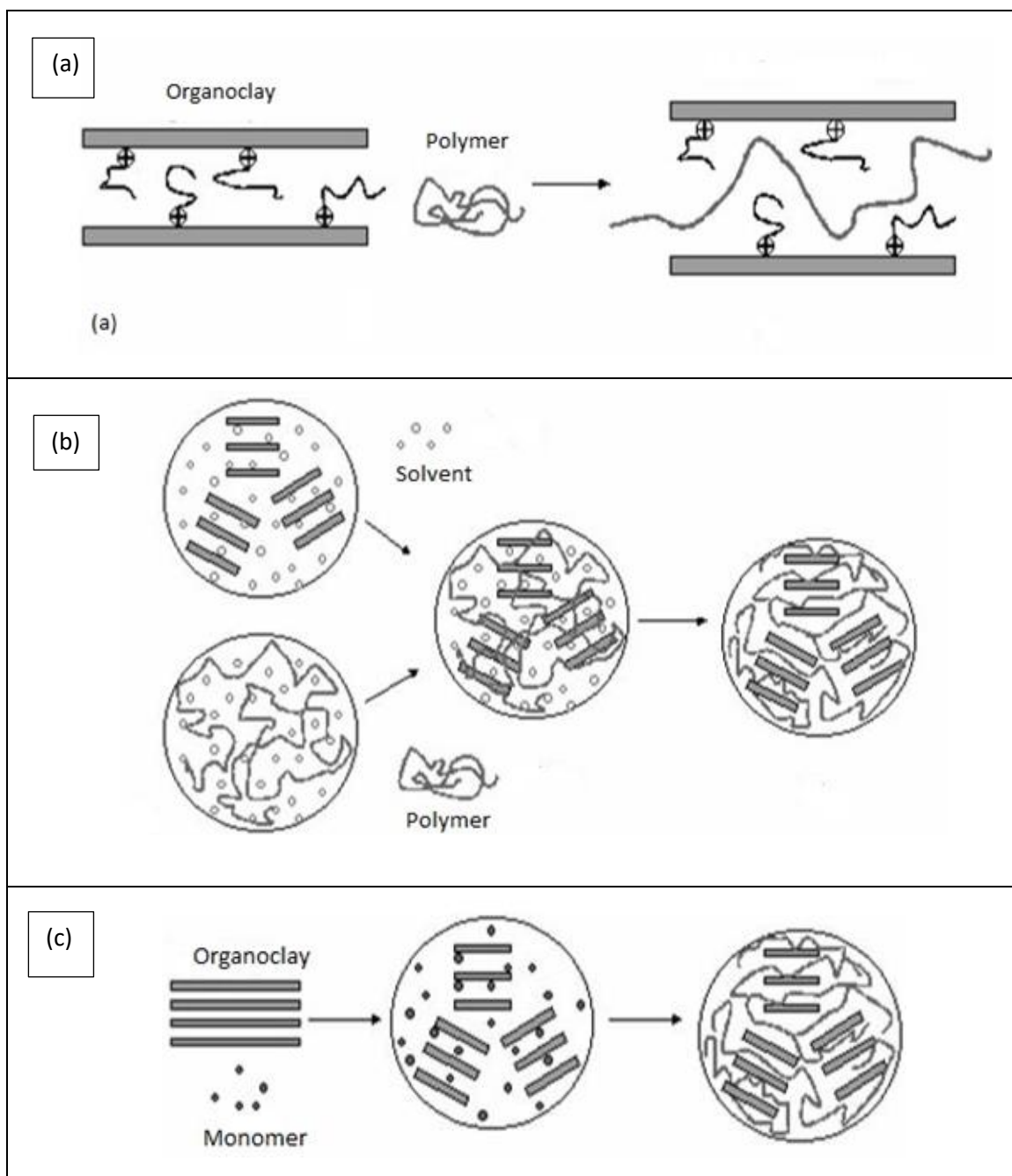
Figure 2.4 :Different methods of PCN preparation (a) melt compounding; (b) intercalation of polymer from solution (c) in-situ polymerization [10]

2.5   Miniemulsion polymerization for PCN's

There are different types of heterophase polymerization such as suspension or emulsion polymerization[25,16,35], with miniemulsion falling under this broad category as well.

Although the first composites were synthesized using emulsion polymerization[11], the use of miniemulsion polymerization is a more relevant option with regard to the PCN's. This is due to the difference in monomer droplet formation between these types of polymerization[36,37].

The miniemulsion process typically consists of an oil phase dispersed in a continuous water phase. With the inclusion of surfactant and co-stabilizer under high shear forces via ultrasound or homogenization mechanisms[38] monomer droplets are formed and stabilized in the range from 50–500nm in diameter as shown in Figure 2.5. This type of polymerization was developed by Ugelstad in the 1970's as a variation of conventional emulsion polymerization[5].

With regard to emulsion polymerization, monomer is transported to an empty micelle by means of diffusion where polymerization takes place thus homogenous and micellar nucleation is dominant. The main difference between the two is the mechanism of particle formation. The monomer droplet is preformed and stabilized in the case of miniemulsion with droplet nucleation being prevalent. The monomer droplets are transported to empty micelles which is the site of polymerization during emulsion polymerization[37].
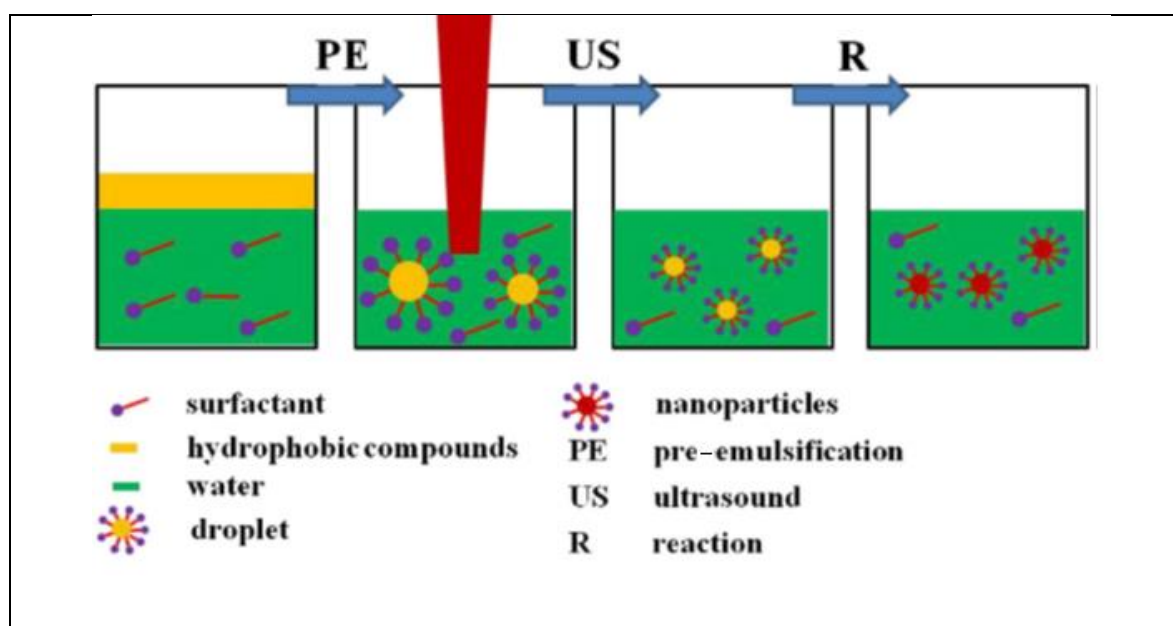
Figure2.5: Schematic overview of the miniemulsion polymerization [5]

The incorporation of inorganic media into a system such as this is favourable since each monomer droplet acts as an independent nanoreactor from the beginning to the end of the reaction[38].

Incorporation by encapsulation of various inorganic materials ranging from titanium dioxide[39] particles, graphene sheets[40] to carbon nanotubes[2] has been integrated into a polymer matrix by using the miniemulsion polymerization technique due to the mechanism of monomer droplet formation as mentioned previously.

These hybrid materials are attractive from an industrial point of view since they offer increased properties in terms of their thermal[12,17], barrier[3] and mechanical properties[41], to name a few, with only a small amount of the inorganic component added.

2.5.1   Highly filled PCNs

According to literature there are not many accounts of large amounts of inorganic media added to the polymer matrix. The most notable being that of Landfester et al. who encapsulated large amounts of carbon black[4] as well as magnetite[42] into a polymer matrix. Other examples include silica particles[6,11] and clay platelets[43]. The application of high clay loadings of PCN's provides an economically viable route in producing a higher quality material as well as an environmentally friendly method of production that can be used in the industry. Zengeni et al.[44] successfully encapsulated up to 50 wt.% Laponite and MMT, respectively, into polymer latexes by using Landfester's[4] technique. However the procedure is only applicable on a small scale. There are a few more opposing accounts of high inorganic loadings with regard to nanocomposites that suggest parameters such as filler dimensions and method of preparation are factors that could affect the superiority of these materials.

2.5.2   Low energy emulsification techniques

Emulsification is an important step in miniemulsion polymerization as it determines the droplet size and the stability of the reaction during polymerization[45]. Additionally, miniemulsions are thermodynamically unstable and kinetically stable which reiterates the importance of this emulsification step [46,47]. Traditional emulsification methods involve high energy input and preclude miniemulsions from being applicable to the commercial sector. However low energy methods have been developed in the past couple of decades as a

solution. They involve taking advantage of the physicochemical properties of the mixture as a function of either temperature or water volume fraction.

The PIT approach involves mixing a mixture of mainly surfactant, monomer and water at room temperature and is then heated gently. As a result, the spontaneous curvature of the dispersion inverts due to minimal surface tension which encourages the assembly of finely dispersed hydrophobic droplets Thus above the PIT, the surfactant is soluble in the oil phase and the emulsion goes through a transition going from an oil-in-water mixture to water-in-oil mixture [33] as seen in Figure 2.6. The variation of this method is whereby the volume fraction of the water increases gradually starting with a water-in-oil emulsion transitions to an oil-in-water dispersion. This technique is referred to as emulsion inversion point (EIP). It involves the gradual addition of the water which causes the curvature of the water to change to oil droplets respectively. Research is based primarily on single component polymer systems with some accounts of intentions to further study the effect of encapsulating thermosensitive substances[48].
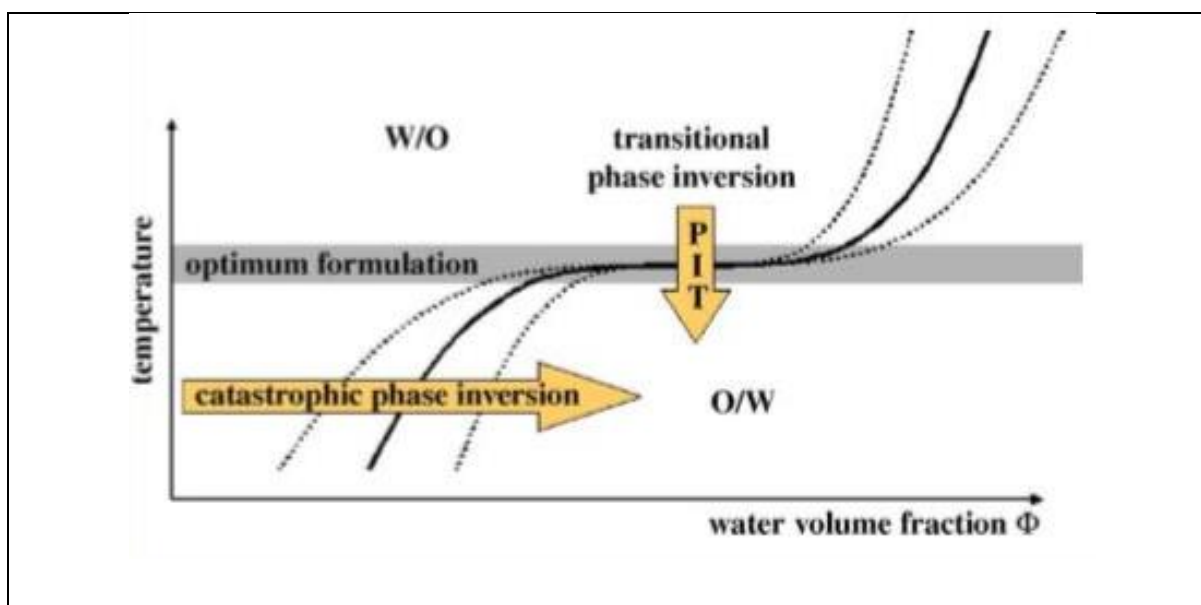
Figure 2.6: Illustration of the difference between phase inversion temperature and emulsion inversion point[45]

2.5.3   Alternative homogenization devices
PCN's have been successfully produced on a lab scale via miniemulsion polymerization and the changes in their properties have been investigated in comparison to the neat polymer,

however, these materials can't be practically produced on an industrial scale using current procedures. The use of emulsification equipment such as a sonicator, which breaks up the oil and water phases by means of cavitation, isn't viable due to its high energy input and volume limitations. There are other alternatives to using sonication[35], these include high pressure homogenizers, rotor stators and in-line mixers[49].

Rotor stators can produce miniemulsions within the required droplet size range but are delicate in terms of viscosity. Further drawbacks to using this device include poor dispersion quality and lack of uniformity with regard to monomer droplet distribution[50,51].

Static mixers offer a low maintenance and low energy alternative in comparison to rotor stators and homogenizers. However long processing times make them undesirable[50].

The most suitable option seems to be high pressure homogenization. It can handle industrial capacity needs, with low processing times. At high solid content, dispersions can be prepared with highly viscous monomer dispersion of nanodroplets[50].

When Ugelstad developed the method of miniemulsion he did not have any of the above mentioned technology available and simply used mechanical stirring.

2.6   Characterization

2.6.1   PCN Morphology:

2.6.1.1   Transmission electron microscopy

The spatial arrangement of the silicate layers within the PCN is significant in terms of relating its influence on the polymer phase to its physical characteristics. Transmission electron microscopy (TEM) provides a qualitative depiction of the degree to which the polymer has penetrated the clay stacks with regard to the wet latex and the dried film. A visual representation of a localized area of the material is used to determine the morphology of the clay in the polymer matrix where a single platelet (Figure 2.7(a)) is visible as well as a tactoid (Figure 2.7 (b)). Although the obvious drawback of this technique is that it is not representative of the bulk sample it can be used in conjunction with a quantitative technique such as X-ray diffraction[52,1].
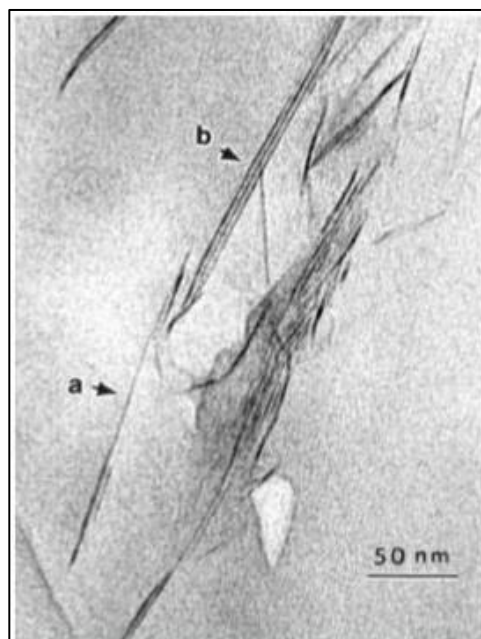
Figure 2.7: (a) an exfoliated sheet and (b) small intercalated tactoid [52]

2.6.1.2   X-ray diffraction

X-ray diffraction (XRD) analysis indicates the structure (exfoliated or intercalated) of the nanocomposite by the observation of the shape, position and intensity of the basal reflections from the layers of platelets and the use of Braggs law [4-8,25],

$$n\lambda = 2d\sin\theta \qquad\qquad \text{\textit{Equation 2.1}}$$

where λ is the wavelength of the X-ray radiation, n:order of interference, d:interlayer distance and θ:diffraction angle. It is a useful way to determine the degree of dispersion of the clay platelets in contrast to the pristine clay. However there are difficulties associated with unclear basal reflections; peak broadening and reduction in intensity are difficult to resolve precisely[6]. Furthermore, small angle X-ray scattering (SAXS) determines the layer spacing when the spaces increase to 6-7 nm or when they become more dispersed in exfoliated structures[6,25]. This is exemplified by the study of melt processed polystyrene/MMT and polypropylene-grafted maleic anhydride/MMT, respectively. These PCN's were analyzed in comparison to the neat MMT and it was clear from Figure 2.8 that the basal spacing shifted with respect to the neat clay and confirmed the exfoliation of the platelets with the increase in basal spacing[52].
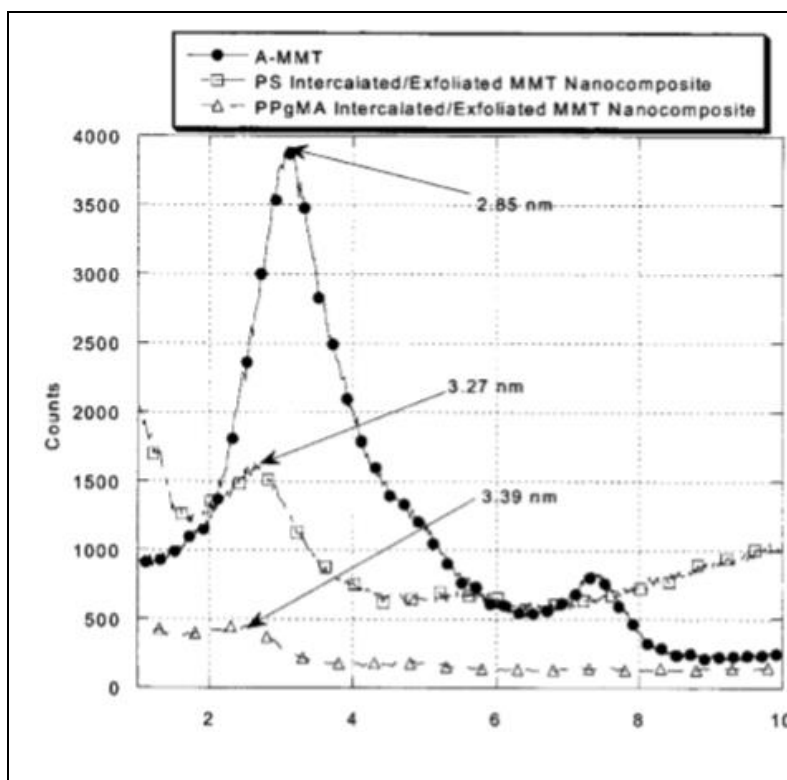
Figure 2.8 :XRD plot of MMT PS and PPgMA nanocomposites[52]

2.6.2   PCN latex characterization:

When heterogeneous polymerization methods are used the particle sizes of the PCNs are of significance and are analysed by dynamic light scattering (DLS). One of the shortcomings of this technique is that the results are skewed towards the larger sized particles due to Brownian motion in the solution. In most cases it is preferential for the monomer and clay to interact which means that they are attached to the surface or encapsulated within the monomer droplet. Thus, particle size must be appropriate[35]. The particle size can also be investigated by TEM to supplement DLS since both analyses are based on different principles. However, a shortcoming of both techniques is that none of them is indicative of the amount of clay present quantitatively in the hybrid material.

2.6.3   PCN physical properties:

2.6.3.1   Thermal properties

Thermogravimetric analysis (TGA) is employed to quantitatively probe the degree to which PCNs as well as organoclay decompose as a function of temperature. Typically, the organic components i.e. the polymer in the PCN and surface modifier in the organoclay will degrade at a much lower temperatures as opposed to its inorganic counterpart. As mentioned earlier,

16

improved thermal stability, which is signified by the increase in onset temperature of the PCNs is observed which is an attractive feature. Although the exact degradation mechanism is unclear it is suggested that the silicate layers are impermeable to gases and thus limit oxygen diffusion which is key factor in thermal degradation[11,23,15].

2.6.3.2   Thermomechanical properties:

The material's response to thermal events such as α-transitions, which are related to the Brownian motion of the polymer chains at the transition from glassy to rubbery state, is also referred to as the glass transition temperature (T_g), and is a direct result of the interaction between the polymer and the clay. The investigation of this and other phenomena is done by using differential scanning calorimetry (DSC) [12]. It is widely reported throughout literature that the effect of clay on PCNs has a positive effect on the T_g in comparison to the neat latex due to segmental mobility of the polymer chains being reduced[12,20]. Although there are opposing studies where a decrease in T_g is observed this is due the plasticization of low molecular weight molecules [30].

The process of degradation in relation to heating is of importance as it is indicative of the stability of the nanocomposite which is characterized by a higher onset temperature. The mechanical behaviour of PCNs are related to the molecular motions of the polymer and its interaction with the platelets which go through different phases (from glassy to rubbery) which is time or temperature dependent. Dynamic mechanical analysis (DMA) translates this information as the loss and storage moduli, respectively. PCNs have shown a dramatic increase in these moduli which is due to the reinforcing nature of the rigid platelet filler. This is exemplified by the melt intercalation of polypropylene/MMT nanocomposites were found to exhibit higher storage and loss modulus, respectively, was observed with up to 5 wt.% clay loading[32,12].

2.6.4   Barrier Properties of PCNs

In applications[20,53-55] where polymeric materials are used to protect substrates (from an external environment, small molecules as well as solvents) the permeability of these systems is one of importance. The polymer is susceptible to the diffusion of these species as a result of the relationship between them which includes the polymer morphology, molecular weight and solubility of the species to name a few. This diffusion can be described by Fick's Law[56],

$$J = -D\frac{\partial C}{\partial x}$$

Equation 2.2

where J is the driven concentration gradient of adsorbed molecules, D is the diffusivity, C is the concentration of diffusing species and x, the space co-ordination measurement to the normal section. Once the concentration of these small molecules are constant their movement through the film is governed by different parameters referred to as diffusion and solubility. The former is a measure of how fast the small molecules move through the film and the latter indicates the amount of the small molecules absorbed. In order to quantify these transport characteristics sorption and permeation experiments, respectively, are of use. Sorption analysis refers to the mass gain of films that have been exposed to a solvent, under constant pressure, that dissolve and diffuses through the film and yields the concentration of the sorbed solvent. Permeation experiments consist of gas being introduced to one side of a film, at constant pressure, and the amount of gas permeated through to the other side of the film is monitored by the change in volume as a function of time[56].

PCNs offer improved barrier properties due the inclusion of the clay. This is due to the fact that the clay platelets are impermeable and have a large aspect ratio, therefore, enforcing an alternative tortuous pathway (Figure 2.9) for gases to escape. This enhancement has been observed with low clay loadings of up to 10 wt.%[53,55]. According to a recent study clay loadings of up to 20 wt.% clay in poly(styrene-co-butyl acrylate) showed that the unfilled polymer performed better than the filled PCN[57]. This was evidenced by water vapour permeation experiments in which the diffusion coefficients decreased as the clay content increased. Furthermore, Picard et al.[54] substantiated this result using polyethylene and polyamide PCNs.
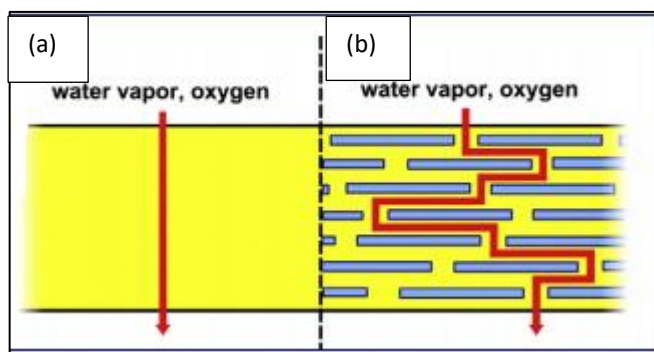
Figure2.9: Illustration of the Tortuous pathway for small molecules in a (a) neat polymer film and (b) PCN film.[55]

2.7   Our approach

The literature discussed in this chapter features the background of PCNs with regard to low inorganic filler contents and the evaluation of their resultant properties. Additionally, the recent research into the field of highly loaded PCNs is also documented. The application of these materials commercially requires reconciliation of resources available in order to produce economically viable and eco-friendly PCNs. Thus it was proposed that the utilization of a high shear mixer be used as the device chosen for emulsification of the immiscible phases in order to create the miniemulsion.

The aim of this study is to incorporate up to 50 wt.% MMT into a PSBA matrix using typical lab procedures and to investigate the structure of the clay within this matrix and their properties. Subsequently, these materials will be experimentally produced using methods that would be of commercial interest. These hybrid materials will be evaluated in terms of their morphological, thermal, and thermomechanical properties.

2.8   References

1.   Hussain, F.; Hojjati, M.; Okamoto, M.; Gorga, R. E. *J. Compos. Mater.* **2006**, 40, 27–32.

2.   Podsiadlo, P; Sup, B.; Kotov, N. A. *Coord. Chem. Rev.* **2009**, 253, 2835–2851.

3.   Schmidt, G.; Malwitz, M. M. *Curr. Opin. Colloid Interface Sci.* **2003**, 8, 103–108.

4.   Tiarks, F.; Landfester, K.; Antonietti, M. *Macromol. Chem. Phys.* **2001**, 202, 51–60.

5.   Qi, D.; Cao, Z.; Ziener, U.; *Adv. Colloid Interface Sci.* **2014**, 211, 47–62.

6.   Costoyas, L.; Ramos, J. ; Forcada, J. *J. Polym. Sci. Part A Polym. Chem.* **2008**, 47, 935–948.

7.   Voorn, D. J.; Ming, W.; Herk, A. M. Van. *Macromol.* **2006**, 39, 4654–4656.

8.   Negrete-Herrera, N.; Putaux, J. L.; & Bourgeat-Lami, E. *Prog. Solid State Chem.* **2006**, 34, 121–137.

9.   Reyes, Y.; Peruzzo, P. J.; Ferna, M.; Paulis, M.; Leiza, J. R. *Langmuir* **2013**, 29, 9849–9856.

10.   Russo, G.M. PhD, Salerno, **2004**.

11.   Pavlidou, S.; Papaspyrides, C. D. *Prog. Polym. Sci.* **2008**, 33, 1119–1198.

12.   Corcione, C. E.; Frigione, M. *Materials (Basel).* **2012**, 5, 2960–2980.

13.   Mittal, V.; *Materials (Basel).* **2009**, 2, 992–1057.

14.   Suin, S.; Shrivastava, N. K.; Maiti, S.; Khatua, B. B. *Eur. Polym. J.* **2013**, 49, 49–60.

15.   Tsai, T.; Lin, M.; Chang, C.; Li, C. *J. Phys. Chem. Solids* **2010**, 71, 590–594.

16.   Faucheu, J.; Gauthier, C.; Chazeau, L.; Cavaillé, J.Y.; Mellon, V.; Bourgeat-Lami, E. *Polymer.* **2010**, 51, 6–17.

17.   Utracki, L. *IEEE Electr. Insul. Mag.* **2010**, 26, 6–15.

18.   Gao, F. *Mater. Today* **2004**, 7, 50–55.

19.   Sun, Q.; Schork, F. J.; Deng, Y. *Compos. Sci. Technol.* **2007**, 67, 1823–1829.

20.   Malucelli, G.; Alongi, J.; Gioffredi, E.; Lazzari, M. *J. Therm. Anal. Calorim.* **2013**, 111, 1303–1310.

21.   Fu, X; Qutubuddin, S. *Polymer* **2001**, 42, 807–813.

22.   Ahmadi, S. J.; Huang, Y. D.; Li, W. *J. Mater. Sci.* **2004**, 9, 1919–1925.

23.   Ray, S. S.; Okamoto, M.; *Prog. Polym. Sci.* **2003**, 28, 1539–1641.

24.   Harvey, C. C.; Murray, H. H. *Appl. Clay Sci. 11* **1997**, 11, 285–310.

25.   Quang, T. N.; Baird, D. G. *Adv. Polym. Technol.* **2007**, 25, 270–285.

26.   Singla, P.; Mehta, R.; Upadhyay, S. N. *Green Sustain. Chem* **2012,** 2012, 21–25.

27.   Samakande, A. MSc, Stellenbosch, **2005**.

28.   Zheng, H.; Zhang, Y.; Peng, Z.; Zhang, Y. *Polym. Test.* **2004**, 23, 217–223.

29.   Negrete-herrera, N.; Putaux, J. L.; David, L.; Bourgeat-Lami, E. *Macromolecules* **2006**, 39, 9177–9184.

30.   Azzam, W. R. *Alexandria Eng. J.* **2014**, 53, 143–150.

31.   Yeniova, C. E.; Yilmazer, U. *J. Appl. Polym. Sci.* **2013**,127, 3673–3680.

32.   Hariprasad, K., and M. Senthilkumar. *Frontiers in Automobile and Mechanical Engineering (FAME), IEEE.*, **2010**, pp. 16-20.

33.   Ray, S.S. and Okamoto, M. *Prog. Polym. Sci*. **2003**, 28, 1539-1641.

34.   Chen, B.; Evans, J. R. G. *J. Phys. Chem. B* **2004**, 108, 14986–14990.

35.   Schork, F. J.; Luo, Y.; Smulders W.; Russum, J. P.; Butté, A.; Fontenot, K. *Adv. Polym. Sci.* **2005**, 175, 129–255.

36.   Van Herk, A. M. "Historical overview of (mini) emulsion polymerizations and preparation of hybrid latex particles." Hybrid Latex Particles. Springer Berlin Heidelberg, 2010. 1-18.

37.   Anton, N.; Benoit, J.P; Saulnier, P. *J. Control. Release* **2008**, 128, 185-199.

38.   Landfester, K.; Weiss, C. K. *Adv Polym Sci* **2010**, 229, 1–49.

39.   Erdem, B.; Sudol, E. D.; Dimonie, V. L.; El-aasser, M. S. *J. Polym. Sci. Part A Polym. Chem.* **2000**, 38, 4419–4430.

40.   Etmimi, H. M. PhD, Stellenbosch, **2012**.

41.   Jordan, J.; Jacob, K. I.; Tannenbaum, R.; Sharaf, M. A.; Jasiuk, I. *Mater. Sci. Eng. A* **2005**, 393, 1–11.

42.   Hoffmann, D.; Landfester, K.; Antonietti, M. *Magnetohydrodyn.* **2001**, 37, 217-221.

43.   Zengeni, E.; Hartmann, P. C.; Pasch, H. *Compos. Sci. Technol.* **2013**, 84, 31–38.

44.   Zengeni, E. PhD, Stellenbosch, **2012**.

45.   Fernandez, P.; André, V.; Rieger, J.; Kühnle, A. *Colloids Surfaces A Physicochem. Eng. Asp.* **2004**, 251, 53–58.

46.   Cheng, S.; Guo, Y.; Zetterlund, P. B. *Macromolecules* **2010**, 43, 7905–7907.

47.   Guo, Y.; Zetterlund, P. B. *Polym.* **2011**, 52, 4199–4207.

48.   Anton, N.; Vandamme, T. F. *Int. J. Pharm.* **2009**, 377, 142–147.

49.   Ouzineb, K.; Lordab, C.; Lesauzec, N; Graillata, C.; Tanguy, Philippe A. T.; McKenna, T. *Chem. Eng. Sci.* **2006**, 61, 2994–3000.

50.   Asua, J. M. *Prog. Polym. Sci.* **2014**, 39, 1797–1826.

51.   Anton, N.; Benoit, J.; Saulnier, P. *J. Control. Release* **2008**, 128, 185–199.

52.   Morgan, A. B.; Gilman, J. W. *J. Appl. Polym. Sci.* **2003**, 87, 1329–1338.

53.   . Messersmith, P. B.; Giannelis, E. P. *J. Polym. Sci. Part A Polym. Chem.* **1995**, 33, 1047–1057.

54.   Picard, E.; Gérard, J. F.; Espuche, E. *Revue d'IFP Energies nouvelles*, **2015**, 70, 237-249.

55.   Duncan, T. V. *J. Colloid Interface Sci.* **2011**, 363, 1–24.

56.   Mai, Y.W.; Yu, Z.Z. Polymer nanocomposites. 2006, Woodhead publishing.

57.   Mittal, V. *Materials*. **2009**, 2, 992–1057.

3   Preparation of Polymer Clay Nanocomposites on the Lab Scale

3.1   Introduction:

PCN's are conventionally produced with low filler contents typically in the range from 1-5 wt%[1–6]. Few accounts exist where high clay loadings have been incorporated into a polymer matrix successfully. Of these reports, different preparation routes have been used such as heterogeneous polymerization[7–9] and melt processing[10].

In order to incorporate high amounts of inorganic filler into a polymer matrix traditional methods used to incorporate low filler contents are not suitable due to the increase in viscosity of the dispersion even when heterogeneous polymerization methods are used. This study is based on the work of Zengeni[8,11] who successfully encapsulated up to 50 wt.% of Laponite clay into polystyrene and poly(styrene-co-butyl acrylate), respectively, to produce stable latexes. A modified miniemulsion procedure referred to as the co-sonication method or ad-miniemulsion polymerization was used. The procedure is outlined in Figure 3.1 where two droplet dispersions were created by stirring them and then sonicating them separately. The dispersions were combined to form a hybrid droplet by fission and fusion processes. It is worth mentioning that the dimensions of Laponite (25nm x 0.92nm) are much smaller compared to that of MMT hence encapsulation is favoured with the former. The same study also reported that encapsulation of MMT in a polystyrene matrix was ineffective and the platelets were found to be on the surface instead of inside of the polymer particles.

The aim of this work is to incorporate clay loadings of up to 50 wt.% relative to the polymer. The chosen polymer matrix consists of a random copolymer of poly(styrene-co-butyl acrylate) with a molar monomer percentage composition of 30:70, respectively, which will be referred to as PSBA. The neat latex and nanocomposites will be referred to as PSBA/MMTX where X is the clay loading. The PCNs were investigated according to their morphological, thermal and thermomechanical properties.
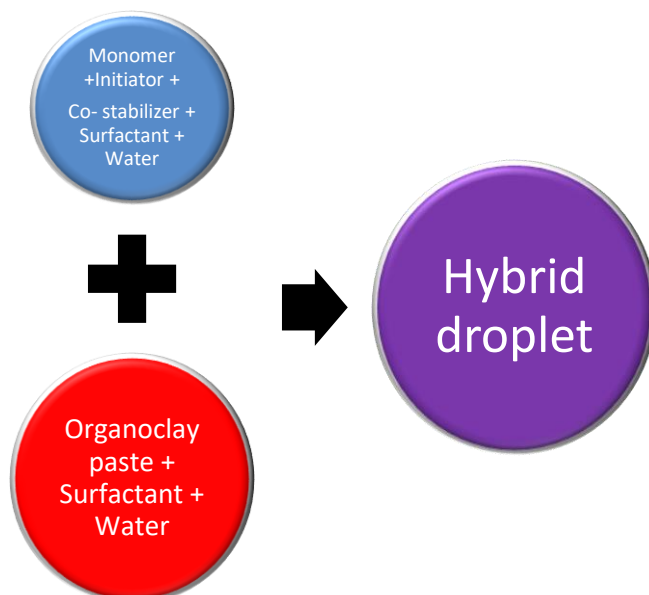
Figure 3.1: *Schematic representation of the co-sonication procedure*

3.2   Experimental:

3.2.1   Materials

Styrene and n-butyl acrylate were supplied by Sigma-Aldrich. N-butyl acrylate was purified by passing through a basic alumina column to remove hydroquinone and monomethyl ether hydroquinone (MEHQ) inhibitors. Styrene was washed successively with a 0.03 M aqueous potassium hydroxide (KOH) solution and distilled water to remove the inhibitor. The washed styrene was then distilled at 40 °C under reduced pressure to remove impurities and possible oligomers which could result from auto-polymerization. Azobisisobutyronitrile (AIBN) was supplied by Sigma-Aldrich and purified by recrystallization from methanol. Montmorillonite (MMT) clay with a CEC of 92.6 meq/100g was supplied by Rockwood Additives Limited, UK. Sodium dodecyl sulphate (SDS, 99%), 4-vinyl benzyl chloride (99%), N,N dimethyldodecylamine (99%), hexadecane (HD, 99%) and silver nitrate ($AgNO_3$) were supplied by Sigma-Aldrich and used as received. Vinylbenzyldodecyldimethylammonium chloride (VBDAC) was synthesized using a method reported elsewhere[5] and its structure was confirmed by ^{1}H NMR spectroscopy.

3.2.2   Surface treatment of MMT

MMT (10 g) was dispersed in 800 mL distilled water. The mixture was stirred for 2 hrs. The organic modifier, VBDAC (4.25g), was dissolved in 200 mL distilled water, and added drop-

wise to the MMT clay dispersion. The mixture was stirred for 24 hr at room temperature. The dispersion was left to stand where two layers formed: a clay rich bottom layer and a water rich top layer. The excess water from the top layer was decanted. The obtained precipitate was recovered by successive centrifugation steps at 3500 relative centrifugal force (RCF) for 5 min. Several washings were done on the obtained precipitate with distilled water until no free organic modifier was detectable using the silver nitrate test (a white precipitate was observed upon addition of a few drops of 0.1 mol silver nitrate to the supernatant). The obtained VBDA-MMT paste was put into a sealable container and stored in a fridge. Powder samples were used to evaluate the extent of modifier grafting onto the MMT clay platelets and were obtained by drying the VBDA-MMT overnight at 45 °C under vacuum.

The modification of MMT was assessed by FTIR and the extent of VBDA grafting was determined by TGA.
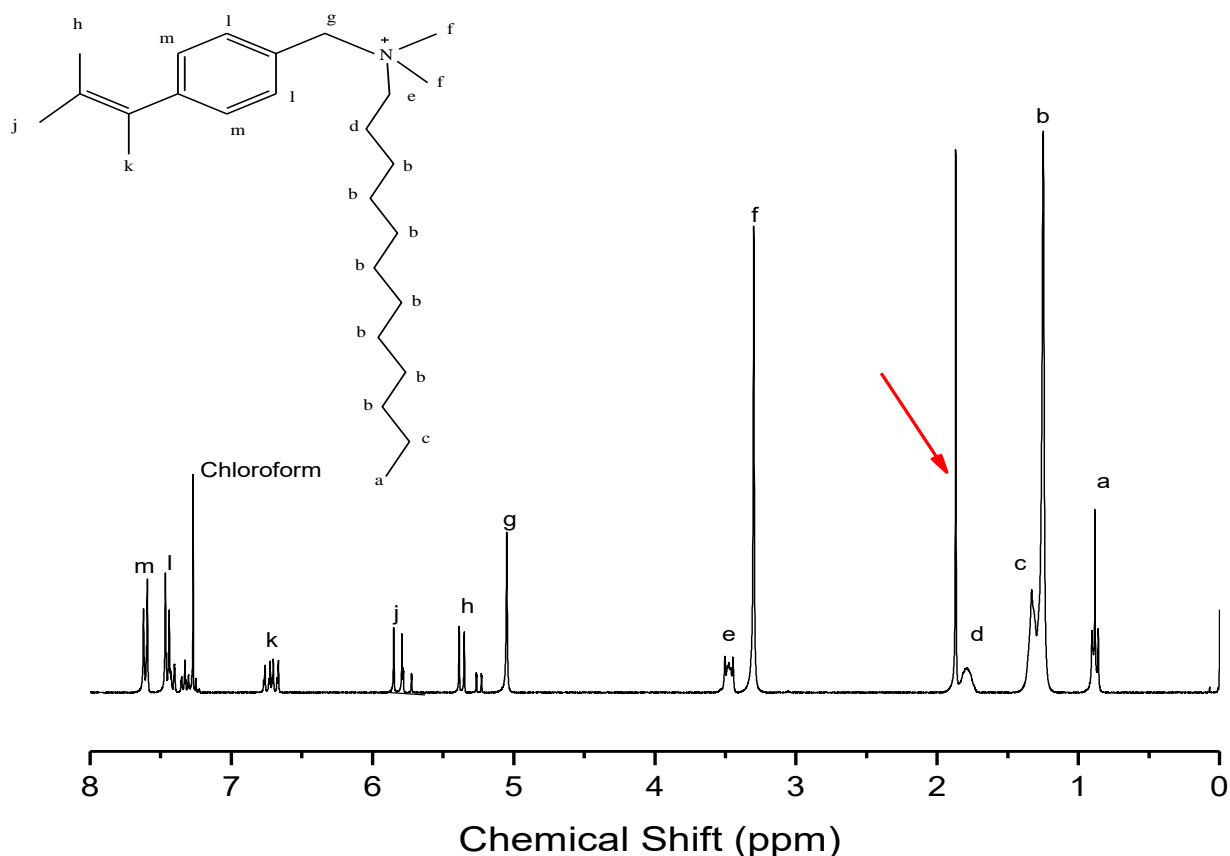
Figure 3.2:VBDAC ^1H NMR Spectrum

3.2.3   Preparation of PSBA MMT Latexes
Aqueous MMT-VBDA dispersions
A particular amount of the VBDA-MMT paste was dispersed in 30 mM aqueous solution of SDS and magnetically stirred for 2 hr. The resulting dispersion was sonicated for 20 min at

90% amplitude and a pulse rate of 5 sec and 1 sec break, exerting 65 ± 5kJ of energy, using a Vibra Cell Autotune series 750VCX high intensity ultrasonic processor (Sonics, U.S.A).

Styrene-butyl acrylate monomer miniemulsions

The monomer miniemulsion was prepared by dispersing monomers of styrene and n-butyl acrylate, AIBN (0.2% relative to monomer) and hexadecane (4 wt.% relative to monomer) in a 10 mM aqueous SDS solution. A molar ratio of 70:30 of n-butyl acrylate to styrene was used. Solids content of 20% for the PCN's was used. The dispersion was stirred for 30 min in an ice bath followed by sonication for 2 min in an ice bath at 50% amplitude without a pulse rate (exerting about 4 kJ of energy). The formulations are presented in Table 3.1.

Table 3.1:PSBA/MMT Formulations

Sample	Aqueous dispersion					Monomer miniemulsion						
	clay (g)	paste (g)	water (g)	SDS (mM)	Water (ml)	BA(g)	S (g)	total (g)	AIBN (g)	HD (g)	SDS (Mm)	Water (ml)
PSBA/MMT00	0	0	0	0	0	5.55	1.95	7.5	0.045	0.3	10	75
PSBA/MMT10	0.75	1.86	1.21	30	49.875	4.995	1.755	6.75	0.0405	0.27	10	25.125
PSBA/MMT20	1.5	4.28	2.78	30	52.5	4.44	1.56	6	0.036	0.24	10	22.5
PSBA/MMT30	2.25	6.43	4.18	30	57.435	3.885	1.365	5.25	0.0315	0.21	10	17.565
PSBA/MMT40	3	8.57	5.57	30	60	3.33	1.17	4.5	0.027	0.18	10	15
PSBA/MMT50	3.5	10	7.5	30	62.55	2.596	0.904	3.5	0.021	0.14	10	12.45

Co-sonication and polymerization

The aqueous MMT-VBDA and the styrene-butyl acrylate dispersions were added together and co-sonicated for 4 min, in an ice bath, at 50% amplitude exerting 10 ± 2 kJ of energy with no pulse. The resultant hybrid miniemulsion was transferred to a three-necked round bottom flask connected to a condenser and a nitrogen inlet, and purged with nitrogen gas for 30 min. The temperature of the oil bath was then raised to 75 °C, and the polymerisation reactions carried out for 4 hr.

Polymer films were prepared by casting 20 mL of latex (10% solids) into glass pans measuring 5 cm in diameter. The samples were allowed to air-dry for about 24 hr. in order to allow film formation, after which they were dried in an oven at 45 °C for a week.

3.2.4   Characterization of the PCN's

FTIR

FTIR measurements were conducted on the dried powder of VBDA-MMT clay using a 1650 Fourier transform infrared spectrophotometer (Perkin Elmer, USA). Thirty two scans were recorded for each sample with a wavenumber resolution of 4 cm^{-1} using the ATR mode.

Sample preparation

About 5-10 mg of the dried powder was placed on the ZnSe crystal sample holder with no further modification.

DLS

A Zetasizer ZS 90 (Malvern Instruments, U.K.) equipped with a 4 mW He-Ne laser, operating at a wavelength of 633.0 nm was used for DLS analysis of the PCN latex samples. The scattered light was detected at an angle of 90°. The final average particle size was obtained from three measurements, each comprising 10–15 sub-runs. The average particle size was calculated using a CONTIN analysis. Prior to analyses the wet latex samples were diluted with deionised water at a ratio of 15:1.

TEM

The obtained latex was diluted with distilled water at a ratio of 5 drops of water per drop of latex. A 3µL aliquot of the diluted latex was transferred by a micropipette onto a 300-mesh copper grid. In order to establish the extent of clay delamination in the PCNs, dried latex samples were embedded in epoxy resin and cured at 60 ℃ for 24 hr. The embedded samples were then ultra-microtomed with a diamond knife using a Reichert Ultracut S ultra-microtome (Leica, Switzerland) at room temperature, thus yielding film sections of about 100 nm thick bright field TEM images were recorded at 200 kV with a Tecnai G220 high resolution TEM (FEI, Netherlands) equipped with LaB$_6$ filament and a Gatan GIF Tridiem post-column energy filter. The image contrast was enhanced by inserting an energy filter of 20 eV in the electron beam path in order to filter out inelastically scattered electrons, which contribute towards background noise in the digitally recorded images.

TGA

Thermograms of dry powder VBDA-MMT clay and PCN samples (10mg) were recorded on a Q500 TGA 7 thermogravimetric analyser (Perkin Elmer, U.S.A). The TGA experiments were

carried out under nitrogen atmosphere at a gas flow rate of 5mL/min. The temperature was increased from 25 °C to 850 °C at a heating rate of 15 °C/min.

DSC

The DSC runs were conducted on a Q100 DSC system (TA Instruments, U.S.A) calibrated with indium metal according to standard procedures. Heating and cooling rates were maintained at a standard 10 °C/min. The samples (6mg each) were first subjected to a heating ramp up to 160 °C, after which the temperature was kept isothermal at 160 °C for 5 min to erase the thermal history. The cooling cycle from 160 °C to -40 °C followed the isothermal stage during which data was recorded.

DMA

DMA measurements were conducted using a Physica MCR 501 rotational rheometer (Anton Paar, Germany) in oscillatory mode. Analyses of PSBA-MMT were performed in the range 10 °C–140 °C. All tests were conducted under 0.1% deformation and a 15 N normal force, with an oscillatory frequency of 1 Hz.

In order to prepare smooth films, the films were melt pressed at 10 Pa and heated to 40℃ for 5 minutes. These films were sectioned into disk shaped films measuring 3 cm in diameter. The thickness of all samples was in the range 200–400 µm.

3.3   Results and discussion:

3.3.1   Surface modification of MMT:

The organoclay produced was analyzed by TGA and FTIR. The former serves as a quantitative and the latter a qualitative measure of the ion exchange reaction between the clay and surfactant. The IR spectra of MMT, VBDAC, and modified MMT are shown in Figure 3.3. The characteristic peaks of each spectrum are highlighted, with the presence of the alkyl chains at 2928 and 2832 cm^{-1} in both VBDAC and MMT-VBDA as well as the aromatic carbons at 1486 cm^{-1} confirm the attachment of the surfactant modifier to the surface of the platelets. The defining peak in the MMT spectra is that of the Si-O peak at 982 cm^{-1} which is also present in the MMT-VBDA. The decrease in intensity of the peak related to the –OH group in the MMT-VBDA which is present in the Na-MMT spectrum is associated with the decrease of water present on the surface. This verifies the ion exchange reaction between VBDAC and neat MMT.
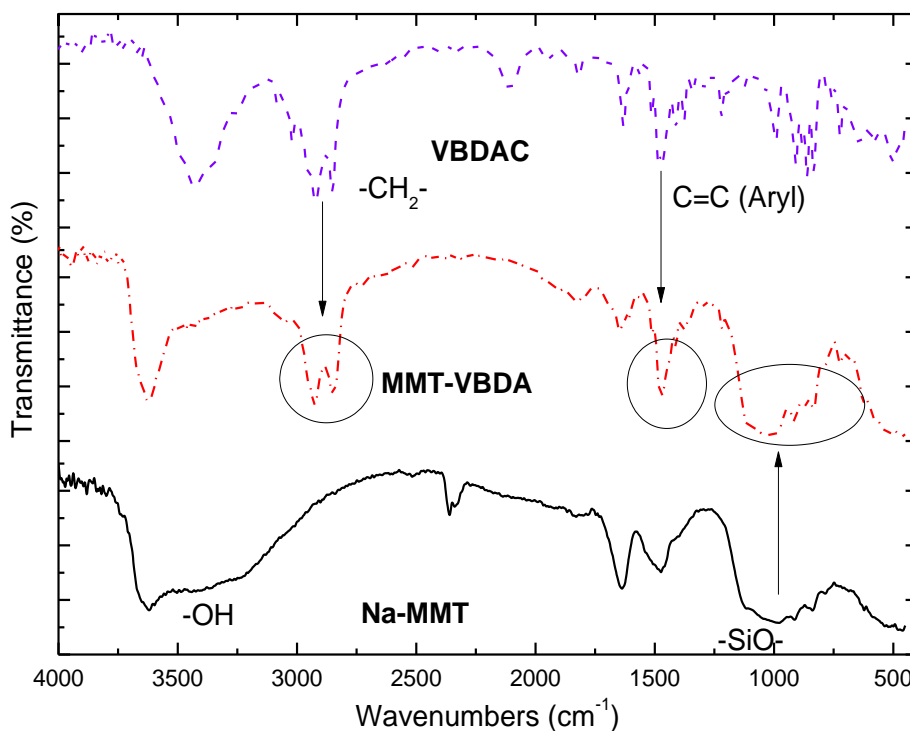
Figure 3.3: *FTIR sprectra of surfactant modifier, organoclay and pristine clay*

The extent of modification was quantitatively determined by TGA. Figure 3.4 shows both the neat MMT, MMT-VBDA (which was modified at 100% CEC) as well as the surfactant modifier (VBDAC).

The neat MMT clay was characterised by one weight loss step between 70 °C and 150 °C [12]. This is attributed to the loss of water adsorbed onto the clay platelets. The inset graph of VBDAC shows a two-step decomposition profile. The first stage between 150 and 300 °C results in the decomposition of the surfactant and the second weight loss step at 350-500 °C is ascribed to decomposed products of thermally induced auto-polymerization of VBDAC. The organoclay showed two weight loss steps where the first step, below 100 °C, is characterised by the loss of adsorbed water. The second step between 250 and 450 °C, is attributed to the decomposition of the surfactant grafted molecules[13]. The amount of modifier attached to the MMT surface was calculated using the residual weight differences between 200 and 600 °C according to Equation 3.1.

$$Amount\ of\ grafted\ surfactant\ =\ \frac{\dfrac{W_{200-600}}{100-W_{200-600}} \times (100 - W_{MMT})}{M} \qquad Equation\ 3.1$$

Where $W_{200-600}$ is the weight loss between 200 °C and 600 °C, W_{MMT} is the weight loss of unmodified clay and M is the molecular weight of VBDAC. According to Equation 3.1 it was found that 87% of the exchangeable sites on the clay surface were successfully modified by the ion exchange reaction.
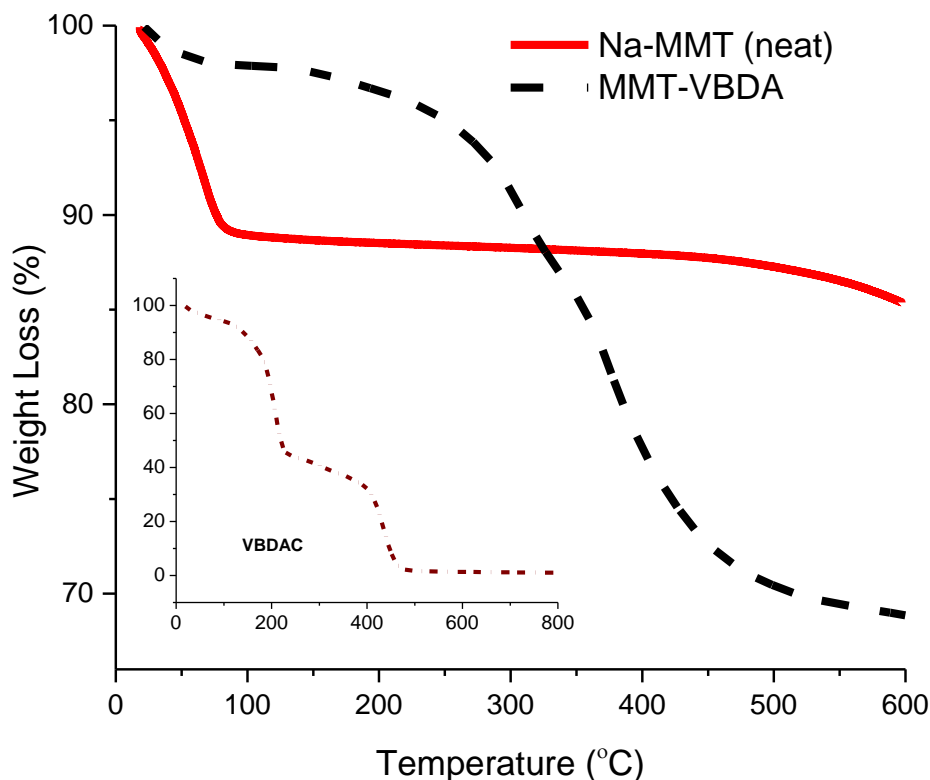
Figure 3.4: Thermograms of Na-MMT (neat), MMT-VBDA and VBDAC (inset)

3.3.2   PSBA/MMT latex characterization

The conversions of monomer to polymer of the prepared latexes were determined gravimetrically in order to determine the effect of clay on the polymerization. As seen in Table 3.1 the conversion decreases as the clay loading increases relative to the neat latex. This can be attributed to the decrease in monomer translational diffusion which is a consequence of increased viscosity with increasing clay content. This behaviour corresponds to literature reports[8].

3.3.2.1   Morphological properties:

PSBA/MMT latexes were produced by miniemulsion polymerization using different concentrations of clay. The wet latex images were observed using TEM in order to determine the structure of the clay in relation to the polymer particles as well as their morphology. The

images of the wet latex are shown in Figure 3.5. The dark areas are representative of the clay platelets since they contain heavy atoms in comparison to the polymer[14].

The neat latex showed spherical particles that were stable with no coagulation present. Subsequently the rest of the clay incorporated latexes showed opposite behaviour with the degree of coagulation increasing as the clay loading increased. Due to coagulation of the latexes the morphology of the clay platelets within the latex as well as the particle size is not clear. However, dumbbell shapes exist for the PSBA/MMT10-PSBA/MMT30 samples which is a possible indication of encapsulation[5,7,15] or platelets lying on the surface of the particles[16]. For PSBA/MMT40 and PSBA/MMT50 heavily coagulated particles were observed thus an inference can be drawn from the images: the collapsed particle morphology is a result of particles agglomerated around the clay compared to the somewhat spherical particles observed in the samples containing less clay. Furthermore there is a trend of spherical particles present throughout the hybrid latexes that appears that looks similar to those in the neat latex   which leads to the assumption that the dispersion of clay within the particles is not completely homogenous.

DLS was used to determine the effect of the clay platelets on the final particle size of the latexes and the results are tabulated in Table 3.2. In comparison to the neat latex the particle size is smaller for some samples e.g. PSBA/MMT10 and PSBA/MMT20, which is in agreement with a previous report[8]. Regarding PSBA/MMT30 it is slightly larger in size than that of the neat latex. This could be due to the interaction of the platelets on the surface of the particle[7,16]. In the case of PSBA/MMT40 and PSBA/MMT50, both are substantially larger than the neat latex and is large for a dispersion according to miniemulsion polymerization theory[17–19]. These results could be due to the following combination of the previous inference where the platelets interact on the surface of the particles. With the increase in the clay fraction compared to polymer the particles adhere to the platelet surface due to the following factor: the clay is encapsulated in these large particles. Due to the platelets being larger (100-200nm) in comparison to the particles they effectively adhere to the platelets which suggests encapsulation amongst these particles [5].
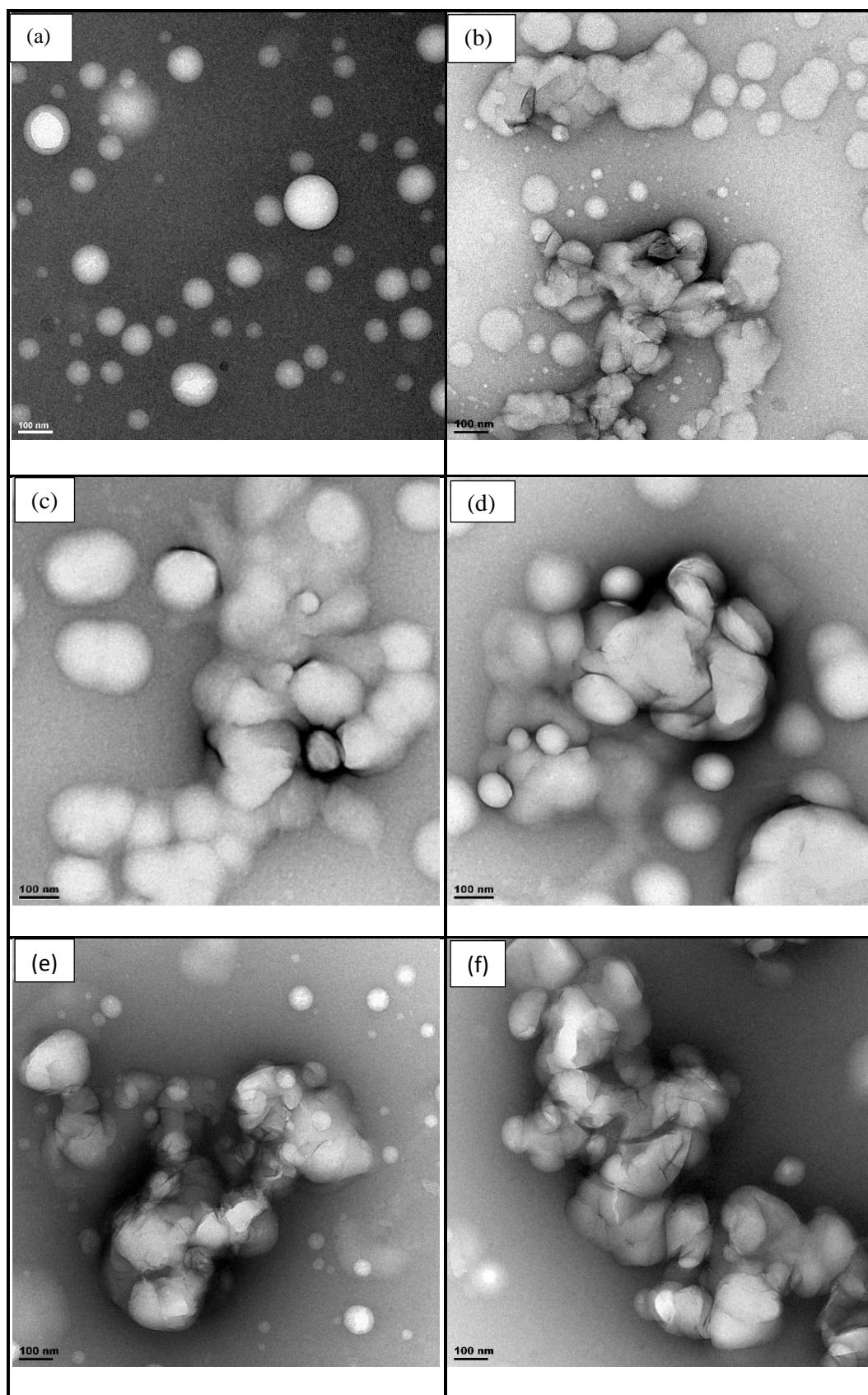
Figure 3.5: *Transmission electron images of (a) PSBA/MMT00, (b) PSBA/MMT10,*

(c) PSBA/MMT20, (d) PSBA/MMT30, (e) PSBA/MMT40, (f) PSBA/MMT50.

Table 3.2: Conversion and Particle size of PSBA/MMT latexes

Sample	Conversion (%)	Average particle size (d. nm)
PSBA/MMT00	94	90
PSBA/MMT10	86	60
PSBA/MMT20	80	54
PSBA/MMT30	77	102
PSBA/MMT40	59	320
PSBA/MMT50	60	726

Dry film morphology:

The film morphology was studied using microtomed samples of the hybrid materials which were imaged using TEM as seen in Figure 3.6.

The dispersion of the platelets can be seen clearly throughout the different samples. There is a trend with the degree of delamination decreasing as the amount of clay increases as expected. The samples show the homogenous distribution of platelets from PSBA/MMT10-PSBA/MMT30. Referring to the last two samples stacks or tactoids are present and can be interpreted as phase separation on the nanoscale of the materials.
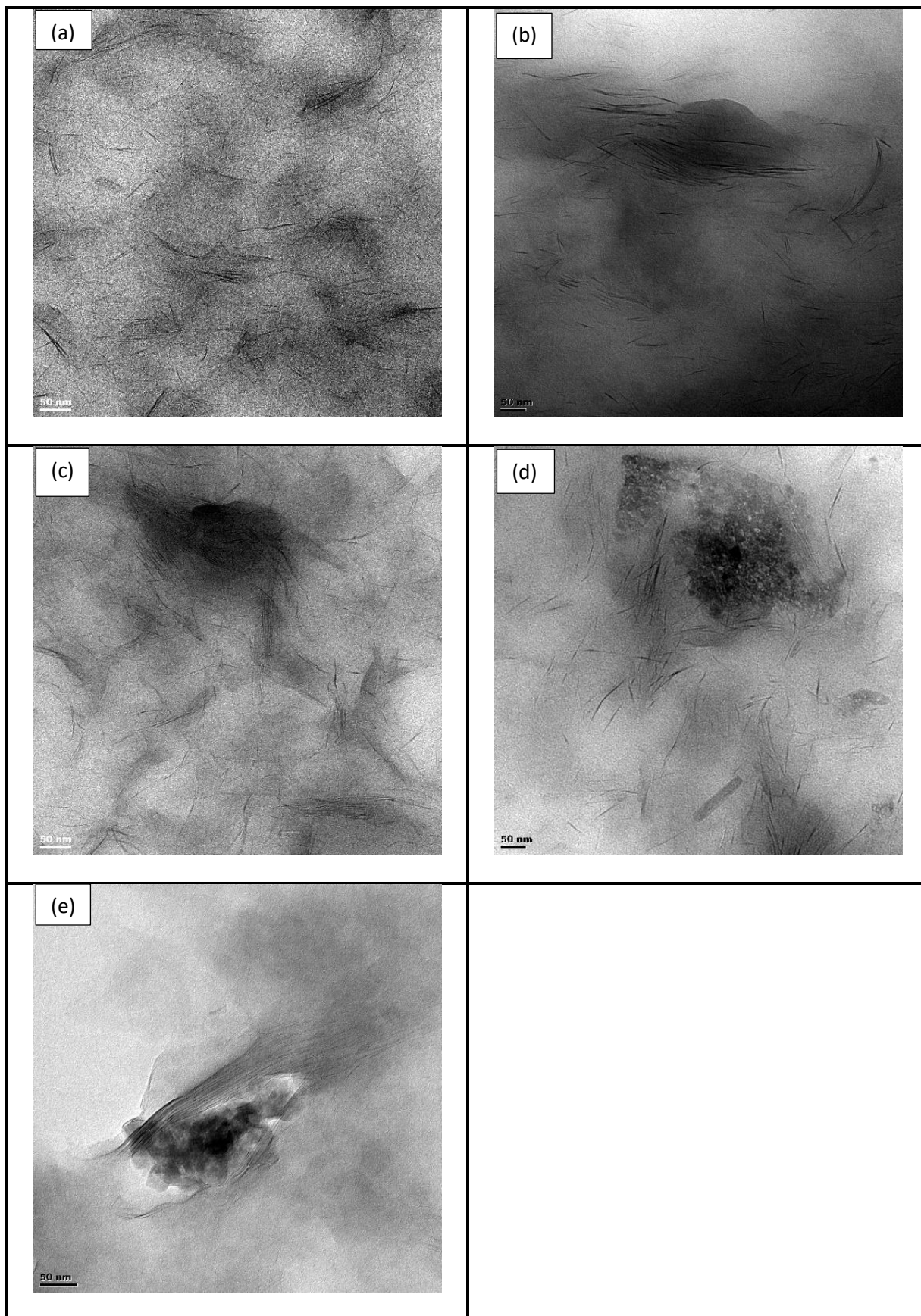
Figure 3.6: Transmission electron images of microtomed (a)PSBA/MMT10, (b)PSBA/MMT20, (c)PSBA/MMT30, (d)PSBA/MMT40, (e)PSBA/MMT50.

3.3.2.2   Thermal stability:

TGA confirmed the amount of clay present in the samples and also validated the method used for calculating the amount of clay required in the formulations. The change in thermal stability of the nanocomposites is marked by the difference in onset temperature as seen in Table 3.3 and Figure 3.7 represents this data. The onset points for the nanocomposite latexes were not clear from the thermograms thus DTG was plotted in Figure 3.8 in order to determine the areas of greatest weight loss which were taken as the onset temperature.

The thermograms show a decrease in thermal stability of the nanocomposite materials in comparison to the neat latex. Furthermore the PSBA/MMT10-PSBA/MMT50 profiles show more than one degradation step. There are two particular degradation steps that are present in the nanocomposite materials. The first arises at a temperature between 200 and 275 °C which is lower than the onset temperature of the neat latex and is minor compared to the second peak observed from 400 to 500 °C of which it overlaps with PSBA/MMT00. The major weight loss step occurs in this range and is reported in Table 3.3 as the onset temperature. As reported in Section 3.3.2 the onset temperature of VBDAC occurs in the range of the first peak of the DTG graph. Thus it can be inferred that the weight loss that occurs at this temperature is that of low molecular weight polymerizable surfactant VBDAC. It is clear that the nanocomposite films with clay loading of up to 40% show an increase in onset temperature. The PSBA/MMT50 sample shows a much lower value as a result of plasticization effects and is more complex due to inhomogeneous incorporation of MMT-VBDA into the polymer matrix during polymerization.
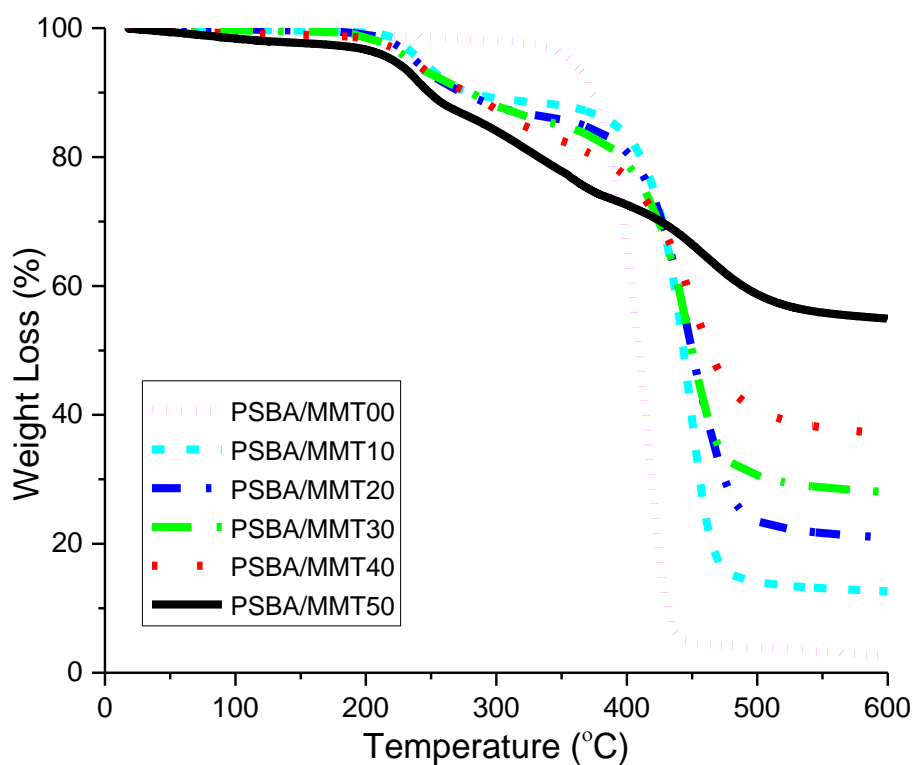
Figure 3.7: *Thermogravimetric profiles of neat PSBA and PSBA/MMT nanocomposite films*
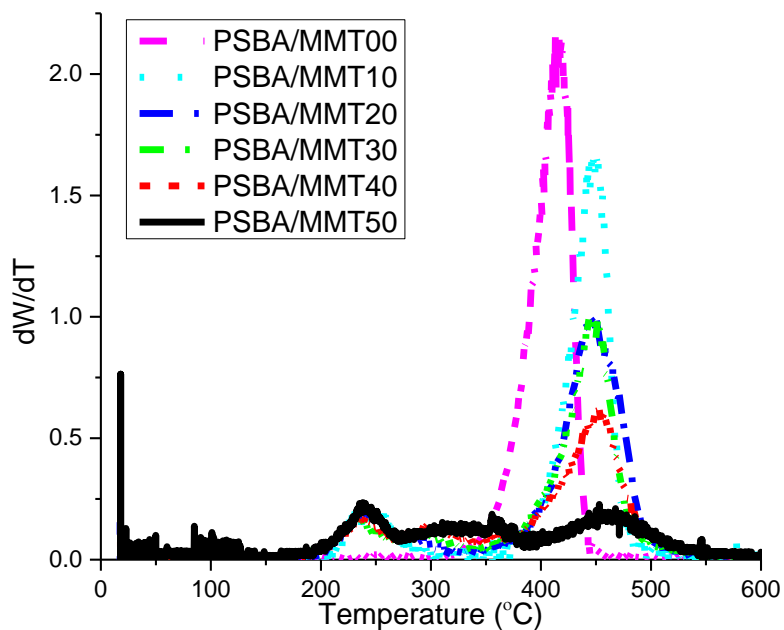
Figure 3.8: *DTG curves of neat PSBA and PSBA/MMT nanocomposite films*

Table 3.3: TGA data of neat PSBA and PCN films

Sample	T_{onset} [a]	m_R [b]
PSBA/MMT00	418.86	1.9
PSBA/MMT10	448.19	12.6
PSBA/MMT20	452.04	20.9
PSBA/MMT30	447.66	28.0
PSBA/MMT40	451.67	37.1
PSBA/MMT50	245.81	54.9

(a) Onset temperature of decomposition (b) Residual weight at 590 ℃

3.3.2.3 Thermo-mechanical properties:

The T_g of the hybrid materials were studied in order to determine what effect the clay had on them. There are conflicting reports on the behaviour of clay on the polymer concerning T_g. An increase in T_g results from the prevention of segmental motions of the polymer chains [20,21] whilst a decrease in T_g, as a result of clay inclusion, is consequent of what is referred to as the plasticization effect[10,16,22].

The theoretical T_g of the neat latex was calculated using the Fox equation Equation 3.:

$$\frac{1}{Tg(PSBA)} = \frac{\frac{m(sty)}{m(sty)+m(BA)}}{Tg(sty)} + \frac{\frac{m(BA)}{m(sty)+m(BA)}}{Tg(BA)}$$ *Equation 3.2*

Where mSty and mBA is the mass of styrene and butyl acrylate in grams (g). They were compared with the experimental values determined from Figure 3.8 and Table 3.3.

Table 3.4: DSC data of neat PSBA and PCN films

Sample	T_g (°C)
PSBA/MMT00	-24.99 (theoretical value: 25.4)
PSBA/MMT10	-22.48
PSBA/MMT20	-19.60
PSBA/MMT30	-20.54
PSBA/MMT40	-23.19
PSBA/MMT50	-33.82

DSC measurements were conducted and according to the heating profiles of the materials in Figure 3.8 there was a marginal increase in T_g in comparison to the neat latex which suggests that the clay platelets either have no effect or they enhance the T_g by means of the clay platelets by limiting the motion of the polymer chains. It is clear that the decrease in T_g with regard to PSBA/MMT50 is related to the presence of large amounts of clay present in comparison to the amount of polymer. The plasticization effect serves as an explanation for the decrease in T_g[10]. The intensities of the transitions become reduced as the clay loading increases which is due to the fact that the platelets inhibit the detection of the polymer chain movement[23].
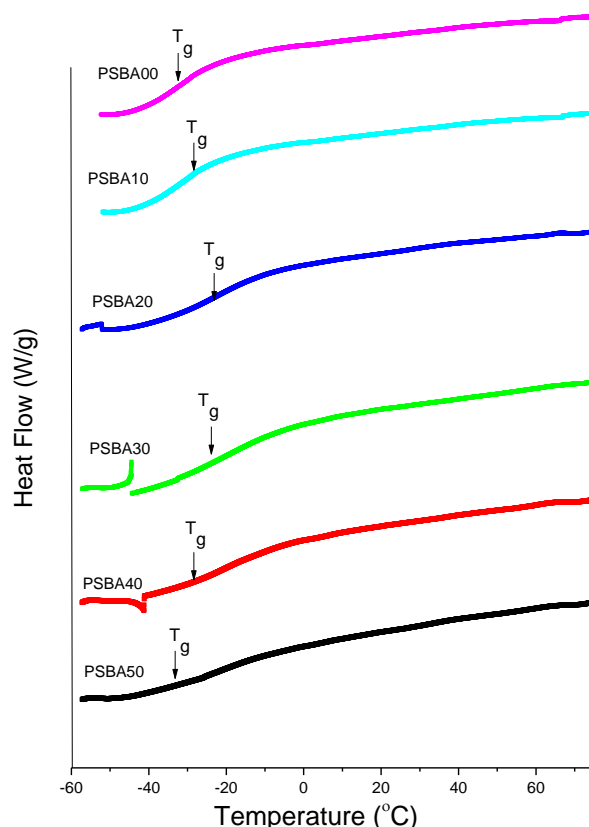
Figure 3.9: *Differential scanning calorimetry heating profiles of neat PSBA and PCN films*

The viscoelastic properties of the materials were evaluated by DMA in terms of their storage and loss modulus, respectively. These results serve as an indication of how the material performs when an oscillating force is applied as a function of temperature.

The samples were prepared by casting films. Once dried they were melt pressed in an effort to obtain continuous and homogenous films. From Figure 3.10 the graphs of the neat latex as well as the PCNs show an increase in storage modulus as the amount of clay increases. Although this result seems to be in accordance with literature, these accounts have used up to 10 wt.% clay. Furthermore this result does not align with those obtained from this chapter.

Recently Murima[9] as well as Zengeni[8] produced highly loaded clay nanocomposites where the opposite behaviour was observed using the same procedure as outlined in Section 3.2.1. This is due to the films being melt pressed before DMA in this study. As mentioned in Section 2.4 the PCNs properties are affected by the method of preparation. There are reports on the effects of melt pressing films in order to produce polymer composites[24–26]. The effect of heat and pressure may have caused crosslinking of the polymer making it tougher[27] and less susceptible to the strain applied to the films and is thus seen to increase as the amount of clay increases[24]. This observation is correlated to the tan (δ) peaks as seen in Figure 3.11 which shows an increase in these peaks as the clay content increases, are close to 0°C with the exception of PSBA/MMT30 which shows a peak height at 17°C. These peaks are related to the T_g of the materials and looking at the DSC results they do not correspond. This could be attributed to the way in which DSC and DMA are obtained. Where the former concerns heating up a sample and tracking the heat capacity over a temperature range which results in a change in heat flow. Whereas DMA tests refer to the sample being subjected to an oscillatory stress and the response to this force is measured. However the films that were used in DMA were compromised as mentioned previously.
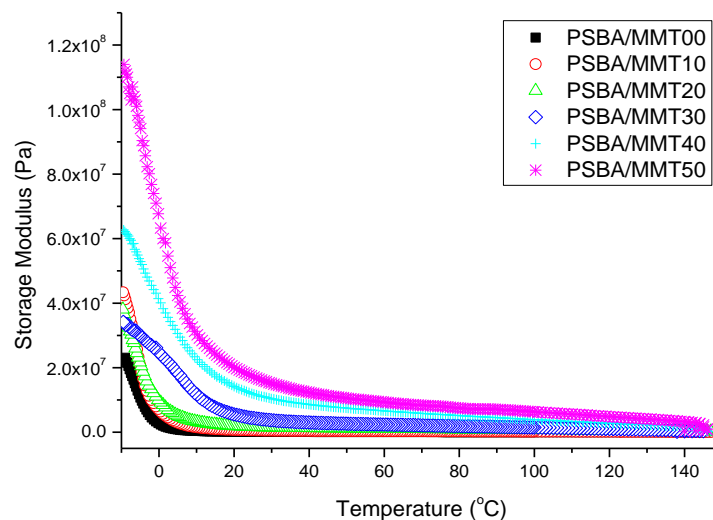
Figure 3.10: Storage modulus of neat PSBA and PSBA/MMT nanocomposite films
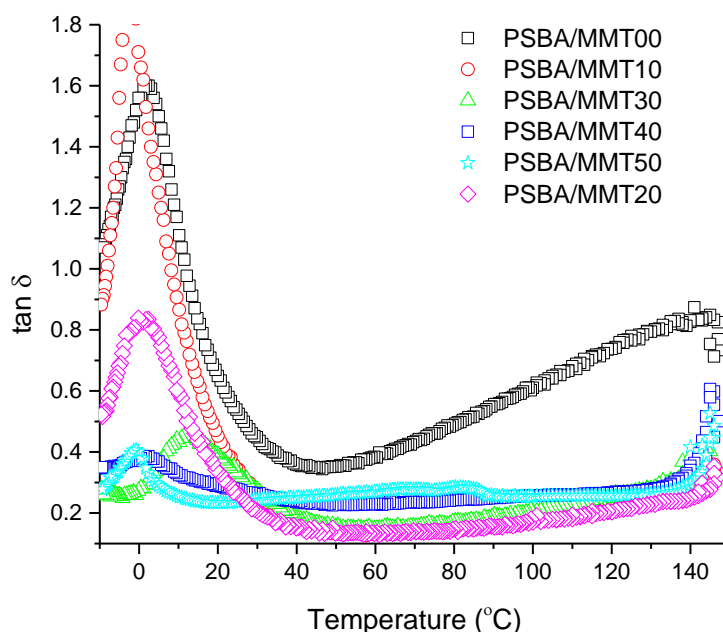
Figure 3.11: Tan (δ) peaks of neat PSBA and PSBA/MMT nanocomposite films

3.4   Conclusion:

The surface modification of MMT was successfully conducted and characterized by both TGA and FTIR confirming the amount of surfactant attached to the platelets as well as verifying this by detecting the presence of key functional groups in the organoclay that are common for both surfactant modifier and clay.

The use of a modified miniemulsion procedure to incorporate large amounts of clay into a polymer matrix proved successful, however, it is clear that going up to higher clay loadings affects the integrity of the material produced which was proven by the analysis of the wet latex which showed coagulated particles by TEM and was further affirmed by DLS.

While TGA confirmed the amount of clay present in the matrix (m_R) a further inference can be made in which the clay paste used suggests that one is able to control the desired amount of clay. The thermal stability of the hybrid materials increased up to 40wt.% clay loading. The highest amount, 50wt.%, showed a much lower onset temperature due to the effect of plasticization mainly. These values were all compared to the neat latex. It must be noted that the nanocomposite thermograms showed a complicated degradation profile which was also due to plasticisation. These weight loss steps were further verified by DTG graphs.

DSC confirmed the premise of the positive influence of clay, however, only up to forty percent clay loading. Higher amounts cause a negative effect in the superior properties as observed for conventionally filled PCNs.

There was an increase in the mechanical properties of the hybrid materials in comparison to the neat latex. This was a consequence of the sample preparation which caused the materials to become tougher due to the crosslinking of the polymer chains.

3.5   References:

1.   Okada, A.; Usuki, A. *Macromol. Mater. Eng* **2006**, 291, 1449–1476.

2.   Azzam, W. R. *Alexandria Eng. J.* **2014**, 53, 143–150.

3.   Quang, T. N.; Baird, D. G. *Adv. Polym. Technol.* **2007**, 25, 270–285.

4.   Negrete-Herrera, N.; Putaux, J. L.; Bourgeat-Lami, E. *Prog. Solid State Chem.* **2006**, 34, 121–137.

5.   Voorn, D. J.; Ming, W.; Van Herk, A. M. *Macromol. Symp.* **2006**, 245, 584–590.

6.   Schmidt, G.; Malwitz, M. M. *Curr. Opin. Colloid Interface Sci.* **2003**, 8, 103–108.

7.   Reyes, Y.; Peruzzo, P. J.; Ferna, M.; Paulis, M.; Leiza, J. R. *Langmuir* **2013**, 29, 9849–9856.

8.   Zengeni, E. PhD, Stellenbosch, **2012**.

9.   Murima, D. MSc., Stellenbosch, **2015**.

10.   Zhang, J.; Jiang, D. D.; Wang, D.; Wilkie, C. A. *Polym. Degrad. Stab.* **2006**, 91, 2665–2674.

11.   Zengeni, E.; Hartmann, P. C.; Pasch, H. *Compos. Sci. Technol.* **2013**, 84, 31–38.

12.   Van Herk, A. M. "Historical overview of (mini) emulsion polymerizations and preparation of hybrid latex particles." Hybrid Latex Particles. Springer Berlin Heidelberg, **2010**. pp 1-18.

13.   Fu, X.; Qutubuddin, S. *Polymer* **2001**, 42, 807–813.

14.   Morgan, A. B.; Gilman, J. W. *J. Appl. Polym. Sci.* **2003**, 87, 1329–1338.

15.   Voorn, D. J.; Ming, W.; Van Herk, A.M.; Bomans, P.H.H.; Frederick, P.M.; Gasemijt, P.; Johanssmann, D. *Langmuir* **2005**, 21, 6950–6956.

16.   Faucheu, J; Gauthier, C.; Chazeau, L.; Cavaillé, J. Y.; Mellon, V.; Bourgeat-Lami, E. *Polymer* **2010**, 51, 6–17.

17.   Schork, F. J. U.; Poehlein, G. W.; Wang, S.; Reimers, J.; Rodrigues, J. *Colloids Surfaces A Physiochemical Eng. Asp.* **1999**, 153, 39–45.

18.   Schork, F. J.; Luo, Y.; Smulders, W.; Russum, J.P.; Butté, A.; Fontenot, K.. *Adv. Polym. Sci.* **2005**, 175, 129–255.

19.   Sood, A. *J. Appl. Polym. Sci.* **2008**, 109, 1262–1270.

20.   Corcione, C. E.; Frigione, M.. *Materials*, **2012**, 5, 2960-2980.

21.   Malucelli, G.; Alongi, J.; Gioffredi, E.; Lazzari, M. *J. Therm. Anal. Calorim.* **2013**, 111, 1303–1310.

22.   García-Chávez, K. I.; Hernández-Escobara, C. A.; Flores-Gallardoa, S. G.; Soriano-Corralb, F.; Saucedo-Salazarb, E.; Zaragoza-Contreras, E. A. *Micron* **2013**, 49, 21–27.

23.   Haraguchi, K.; Li, H. *Macromolecules* **2006**, 39, 1898–1905.

24.   Lee, C.F.;Chen, Y.H.; Chiu, W. Y. *Polym. J.* **2000**, 32, 629–636.

25.   Haggenmueller, R.; Gommans, H. H.; Rinzler, A. G.; Fischer, J. E. **2000**, 330, 219–225.

26.   Kirsch, S.; Doerk, A.; Bartsch, E.; Sillescu, H.; Landfester, K.; Spiess, H. W.; Maechtle, W. *Macromolecules* **1999**, 32, 4508-4518.

27.   Tillet, G., Boutevin, B.; Ameduri, B. *Prog. Polym. Sci.* **2011**, 36, 191–217.

4   Production of PCN's on a Pilot Scale

4.1   Introduction:

PCNs have gained commercial interest since the Toyota group managed to incorporate a small percentage of clay into a polymer matrix which exhibited increased physical, thermal and mechanical properties compared to that of the neat polymer. For this reason these materials have gained relevance in the automotive, packaging and coatings applications[1].

Reports of high filler levels of clay in the polymer matrix are scarce. Laponite[2,3] has been the choice of filler due to its dimensions. The addition of up to 50 wt.% of Laponite clay relative to the polymer weight produced stable superior nanocomposites in terms of physical properties. Adapting it to industrial needs, however, is challenging. Melt processing methods have been employed in order to process these hybrid materials on an industrial scale[4]. Nevertheless there are disadvantages to using this method such as limitation of monomer choice, end use as well as environmental concerns. In this chapter a scaling up of the lab process of the PCNs using heterogeneous polymerisation methods will be reported.

One of the reasons for the scarcity of highly filled PCNs is due to what is referred to as a percolation threshold[5]. It is defined as the minimum amount of inorganic filler that can be incorporated into the nanocomposite that enhances the properties of the said material[5,6]. Thus, although the enhanced properties may not be a feature of these highly loaded materials they can provide an economical option in industry as well as being environmentally sustainable.

The utilization of these PCNs requires production on a larger scale and thus requires a scaling up procedure which occurs in three steps:

1.   Small scale reactions produced in volumes of up to 3L (lab scale production)
2.   Medium sized reactors produced in volumes of up to 50L (pilot size production)
3.   Large metal reactors produced in volumes of up to 20 000L (industry scale production)

This thesis is concerned with going from lab scale to pilot production, respectively. The list above is merely a guide and the lab scale volume used in chapter 3 was 75ml and the pilot size, in this chapter, was 1L. This was done in order to utilize the resources appropriately. Thus the variables and process parameters need to be adjusted accordingly.

The strategy to produce these materials to make them industrially relevant is to use the experimental approach reported in Chapter 3, with alterations. The key step in creating a miniemulsion is the emulsification of the two immiscible phases namely a water and oil dispersion [7,8]. This can be accomplished on pilot scale by imparting mechanical energy in the form of sonication or homogenization with the latter being more commercially relevant[9,10]. An alternative route to perform this step is proposed which is by using a mixer called a Cowles disperser as shown in Figure 4.1 (a) which is available in most manufacturing plants.

A disperser works on the principle of energy transfer. A disc type blade is mounted at the bottom of the mixing shaft and rotated at a relatively high tip speed. (This is the speed at the outer tip or edge of the rotating disc). The solids and liquids are drawn into the rotating disc by the suction it creates. This suction usually results in a visible whirlpool from the top of the mixture down to the top of the disc. A similar whirlpool is created below the disc extending from the bottom of the tank to the underside of the disc. The whirlpools are actually two individual vortices, although common industry practice refers only to the visible upper one known as the vortex. The operating conditions can be seen in Figure 4.1 (b) which is used as a guideline for optimal dispersion.

(a)   (b)
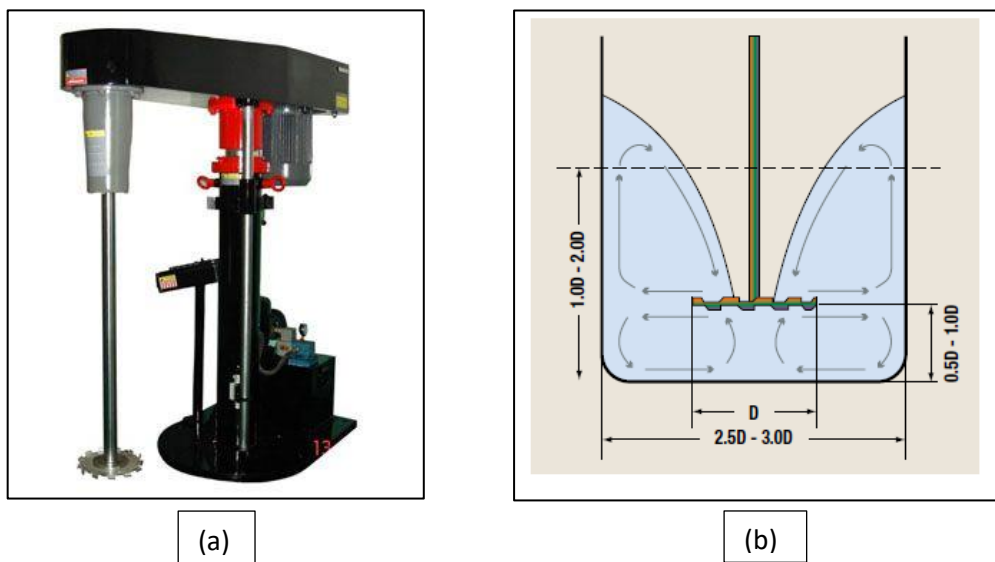
Figure 4.1(a) *Cowles Disperser and (b) operating conditions of the disperser*

The same formulations for the neat as well as the hybrid latex were used also referred to as PSBA/MMTX where X denotes the clay loading with regard to the latex. However due to the cost implications of the large volumes required in the scaling up procedure the use of

surfactant, VBDAC (used in chapter 3), was replaced with an alternative, commercially available surfactant, cetyltrimethylammonium bromide (CTAB).

4.2   Experimental:

4.2.1   Materials

In order to simulate industrial conditions, styrene and butyl acrylate purchased from Sigma Aldrich were used without further purification. Azobisisobutyronitrile (AIBN) was supplied by Sigma-Aldrich and purified by recrystallization from methanol. Montmorillonite (MMT) clay with a CEC of 92.6 meq/100g was supplied by Rockwood Additives Limited, UK. Sodium dodecyl sulphate (SDS, 99%), hexadecane (HD, 99%) and silver nitrate ($AgNO_3$) were supplied by Sigma-Aldrich and used as received. CTAB was obtained from Sigma Aldrich.

4.2.2   Surface treatment of MMT

Large volumes of organoclay were required thus the ion exchange reaction was modified in order to use time and resources more efficiently. Additionally, since the production of the polymerizable surfactant VBDAC is a time consuming and exhaustive procedure, it was decided that CTAB would be used, which is a non-polymerizable surfactant that is commercially available and inexpensive.

Na-MMT was dispersed in distilled deionised (DDI) water (6.25% solids) and was placed on a Cowles disperser at 1500 rpm for 2 hours. CTAB (100% CEC) was dissolved in 100 mL DDI water and added dropwise to the clay dispersion whilst mixing. This dispersion was then filtered under vacuum whilst stirring to remove excess surfactant that was not attached to the surface. Several washings were done on the obtained precipitate with distilled water until no free organic modifier was detectable using the silver nitrate test (a white precipitate was observed upon addition of a few drops of 0.1 mol silver nitrate to the supernatant). The obtained CTAB-MMT paste was put into a sealable container and stored in a fridge. Powder samples were used to evaluate the extent of modifier grafting onto the MMT clay platelets were obtained by drying the CTAB-MMT overnight at 45 °C under vacuum.

The modification of MMT was assessed by FTIR and the extent of CTAB grafting was determined by TGA.

4.2.3   Preparation of PSBA/MMT Latexes

The MMT-CTAB and DDI water were added to a reaction vessel and stirred at 500 rpm on a Cowles Disperser. In a separate beaker styrene, butyl acrylate, AIBN and HD were stirred magnetically. This dispersion was added dropwise to the clay mixture. SDS was dissolved in water separately and added dropwise at 300 rpm into the monomer clay dispersion. This dispersion was stirred for 30minutes at 500 rpm. It was added into a 1 L glass reactor equipped with stirrer blade and polymerized at 70 °C in a water bath for 4 hrs with stirring at 250 rpm.

Table 4.1: Scaled Up PSBA/MMT Formulations

Sample	Aqueous dispersion				Monomer miniemulsion						
	clay (g)	paste(g)	water (g)	Water (g)	BA(g)	S (g)	total (g)	AIBN (g)	HD (g)	SDS (mM)	Water (g)
PSBA	0	0	0	0	74	26	100	0.2	4	25	1000
PSBA/MMT10	10	13.21	3.212	748.75	66.6	23.4	90	0.18	3.6	25	251.25
PSBA/MMT20	20	26.42	6.424	775	59.2	20.8	80	0.16	3.2	25	225
PSBA/MMT30	30	39.64	9.363	824.35	51.8	18.2	70	0.14	2.8	25	175.65
PSBA/MMT40	40	52.85	12.85	850	44.4	15.6	60	0.12	2.4	25	150
PSBA/MMT50	50	66.06	16.06	875.5	37	13	50	0.1	2	25	124.5

4.2.4   Characterization of the PCN's

The latexes and the film morphology of the PCNs were analysed using TEM. The extent of modification was qualitatively confirmed by FTIR and the amount of grafted modifier was quantitatively determined using TGA. TGA was also used to evaluate the thermal stability and to quantify the amount of clay in the PCNs. The PCNs thermomechanical properties were determined by DMA. The T_g of the PCNs was determined using DSC. The detail for these procedures were similar to those reported in Section 3.2.4. Conditions similar to those used for PSBA/MMT PCNs were used in the current study.

4.3   Results and discussion:

4.3.1   Surface modification of MMT:

The structural changes that occurred by the chemical modification of the clay platelet surface were identified using FTIR. The cationic modifier, CTAB, was exchanged with the sodium ions on the platelet surface with the use of a disperser. The characteristic peaks present in the

spectra of Na-MMT, CTAB and MMT-CTAB are assigned in Table 4.1 and the spectrum is shown in Figure 4.2. The structure of the surfactant corresponds to its spectrum. The asymmetrical and symmetrical stretching vibrations of alkyl groups of CTAB are also present in MMT-CTAB. -SiO- and -OH bands were found in Na-MMT corresponding to those found in the MMT-CTAB spectrum[11,12].

The efficiency of the ion exchange reaction of the neat MMT and CTAB to produce the organoclay, MMT-CTAB, was investigated using TGA. As seen in Figure 4.3 (inset graph) the degradation is a one weight loss step between 200 °C and 300 °C which is due to the bulk CTAB decomposition[13]. In order to verify the amount of surfactant modifier attached to clay platelets this was done as mentioned in Section 3.3. According to equation 3.1 the amount of surfactant attached to the platelets was calculated as 67%. Thus this method is not as efficient as the standard ion exchange procedure as outlined in section 3.2. Furthermore previous accounts of surfactant quantities attached to platelet surfaces were higher[2,14].
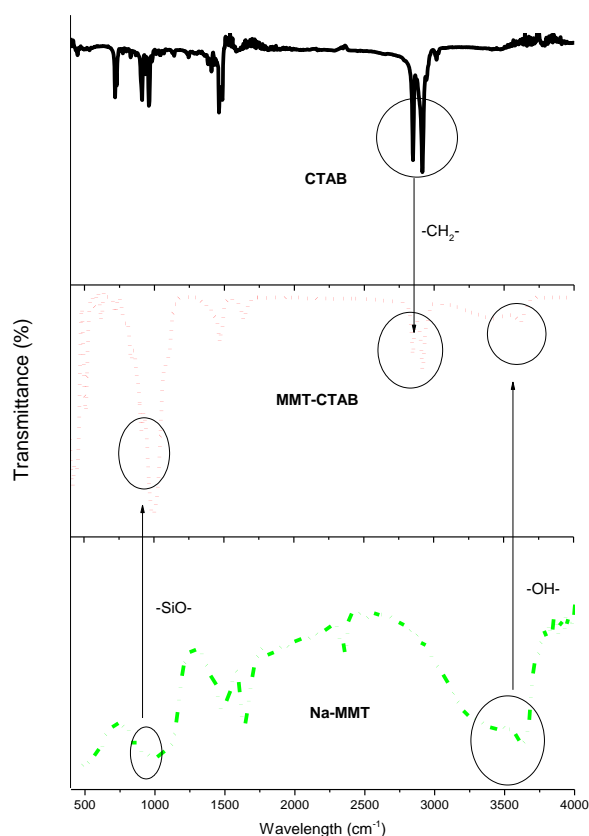

Figure 4.2: FTIR spectra of surfactant modifier, organoclay and pristine clay

Table 4.2: FTIR results of neat MMT, surfactant and organoclay

Assignments	Na-MMT (cm^{-1})	CTAB (cm^{-1})	MMT-CTAB (cm^{-1})
-OH	3447	-	3626
-SiO-	982	-	980
-CH$_2$-	-	2922, 2852	2924, 2851
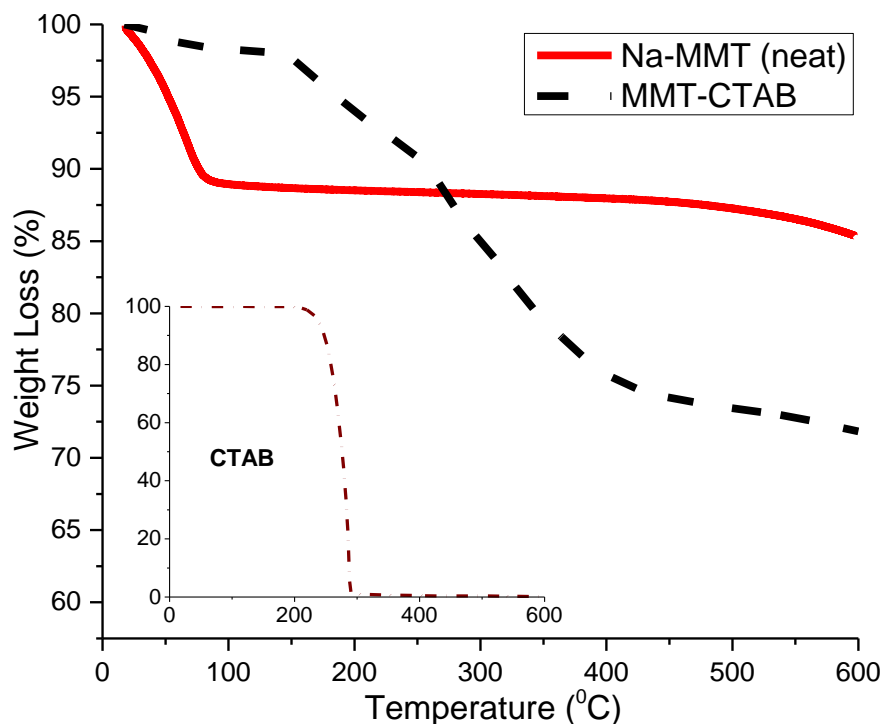
Figure 4.3: Thermograms of Na-MMT (neat), MMT-CTAB and CTAB (inset)

4.3.2   *Characterization of PSBA/MMT latexes:*

The conversions of monomer to polymer of the materials were determined by gravimetric methods and tabulated in Table 4.2. As expected the neat latex exhibited the highest conversion whereas the hybrid latexes showed no particular trend when it came to the dependency on clay loading. Bonnefond et al[15] studied the heterophase polymerization kinetics of nanocomposites using methyl methacrylate (MMA) and BA at clay loadings of up to 3 wt.% and found that a decrease in the rate of polymerization attributed to the difference in hydrophobicity of the monomers influences the intercalation with the clay. The interaction of styrene was favoured over BA in this case due to the former being less polar and thus more compatible with the organoclay.

4.3.2.1 Morphological properties

Using different concentrations of clay the PSBA/MMT latexes were prepared using the procedure outlined in Section 4.2. The images of the neat as well as the nanocomposite latexes are shown in Figure 4.3. As can be seen from Figure 4.3 (a) the neat latex showed spherical particles, however, there are areas where non-spherical particles are observed. This indicates that the neat latex itself is not as stable as the one produced in Chapter 3 or by conventional methods[16]. From Figure 4.3 (b) – (f) the hybrid latex images are unstable in the wet state with regard to particle morphology. There is a large degree of coagulation which increases as the amount of clay content increases (although at the time of analysis the latexes looked homogenous upon visual observation). This is attributed to an increase in clay content meaning a significant increase in viscosity which affects stability of the dispersion during polymerization which increases platelet to platelet interaction which increases the effective volume fraction of particles and coagulation risk is higher[17].

Table 4.3: Conversion and particle size of PSBA/MMT latexes as determined by DLS

Sample	Conversion (%)	Average Particle size (d. nm)
PSBA /MMT00	96	107
PSBA /MMT10	80	80
PSBA /MMT20	91	86
PSBA /MMT30	80	160
PSBA /MMT40	77	500
PSBA /MMT50	78	800

Additionally the platelets are not observable in the images. This is due to the preparation technique that is employed for TEM analysis which can damage the latex. Additionally it is much easier to observe exfoliated structures as opposed to intercalated ones due to the power of the electron beam in use[18]. In this case intercalated structures are expected as opposed to exfoliated ones due to the amount of CTAB attached to the platelet surface which is lower than expected as discussed in Section 4.3.1[19]. Although there are large amounts of coagulation present there is also a proportion of spherical particles that did not interact with the clay. This observation has been reported in literature and is due to the incompatibility of the clay and monomer[20]. However the assumption can be made that the areas of coagulation contain clay platelets[21,22].

Nanocomposite films were prepared and analysed in order to determine the structure of the clay platelets within the hybrid films. The dispersion of the platelets is clearly seen in the

polymer matrix. As the clay content increased exfoliated platelets can be found as seen in Figure 4.4 (a) and (b) and eventually stacks are more prevalent (in Figure 4.4(c-e)) which confirms the inefficient dispersion of the clay platelets as discussed previously. Furthermore the stability of these samples decreases as the amount of clay present in the polymer matrix increases which is substantiated by TEM images as well as the particle size measurements from DLS. The surfactant, CTAB, used in the surface modification of the clay also attributes to this decrease in stability due to its inability to interact with the polymer as efficiently as VBDAC (which is polymerizable) in Chapter 3.

4.3.2.2   Thermal stability:

The latex films were analysed in order to determine their resistance to decomposition with regard to temperature. The performance of the hybrid materials was compared to the neat latex.

The thermograms in Figure 4.6 also provided secondary information regarding the levels of filler present in the matrix with regard to polymer which is available in Table 4.3. All of the materials show a one-step weight loss with the exception of PSBA/MMT50. This is attributed to the heterogeneous dispersion of clay platelets in the films as seen in the previous section. Factors such as monomer conversion as well as amount of surfactant present with respect to monomer also play a role and are visible in the profile. Theoretically the onset temperature is influenced by the platelets that prevent diffusion of volatile decomposition products[12], however, due to this heterogeneity of the tactoids in the polymer matrix there are inconsistent areas. These sections consist of more polymer or clay present which is evidenced by the bumpy thermogram. In order to determine the onset temperature the DTG graph was plotted in Figure 4.6; the nanocomposite latexes decompose all at the same temperature although there are small peaks between 200 °C and 300 °C indicating that there are decomposition products that occur before the stated onset values with the exception of PSBA/MMT40 which shows a notable prior decomposition step at 350 °C and PSBA/MMT50 which also shows a similar profile. The first peak is larger and thus it was reported as the onset temperature. Thus there is no increase in thermal stability with the highest clay containing nanocomposite showing a much lower onset temperature.
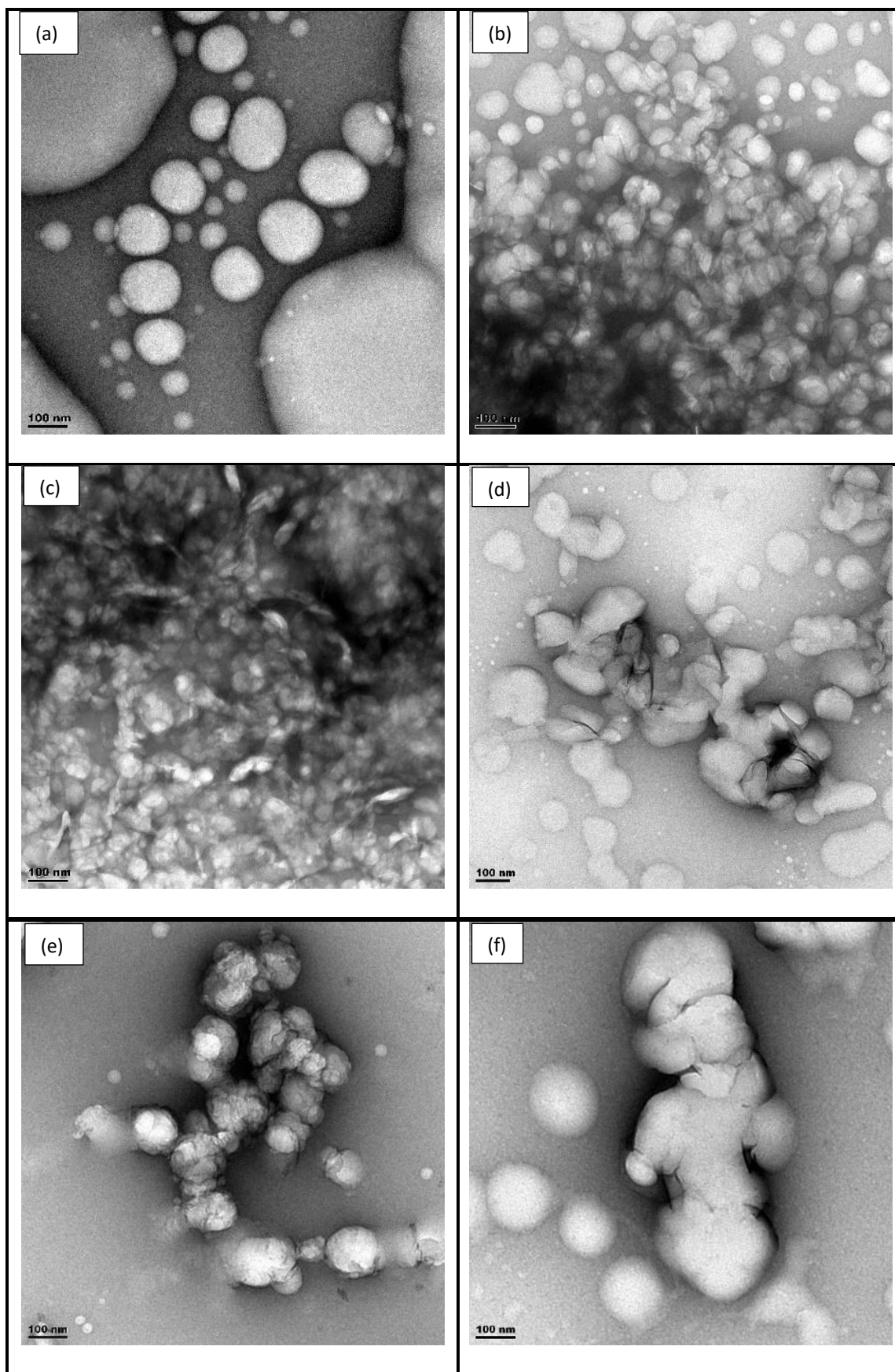
Figure 4.4Transmission electron images of (a) PSBA/MMT00, (b) PSBA/MMT10, (c) PSBA/MMT20, (d) PSBA/MMT30, (e) PSBA/MMT40, (f) PSBA/MMT50.
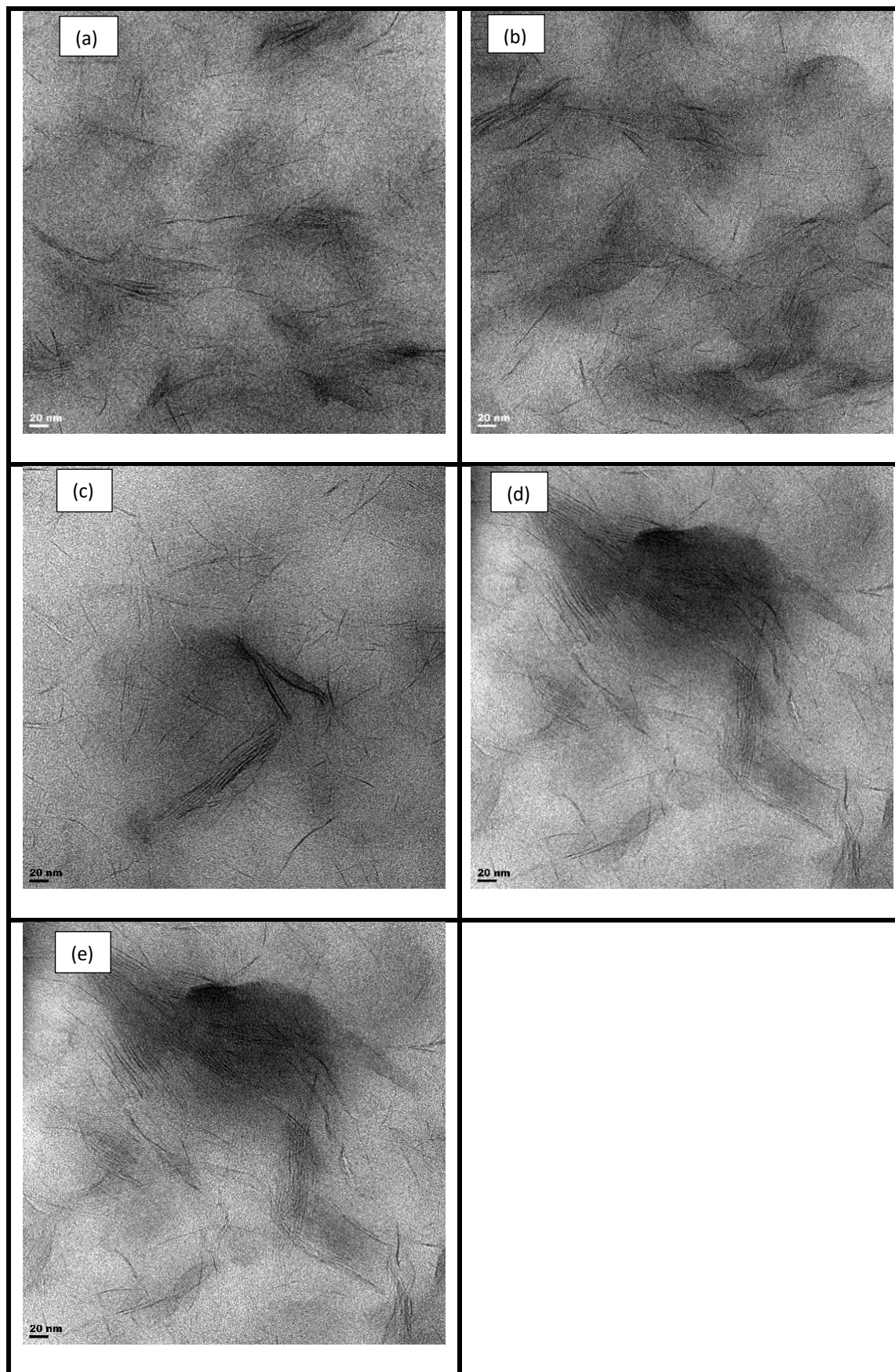
Figure 4.5: *Transmission electron images of microtomed ((a) PSBA /MMT10,*

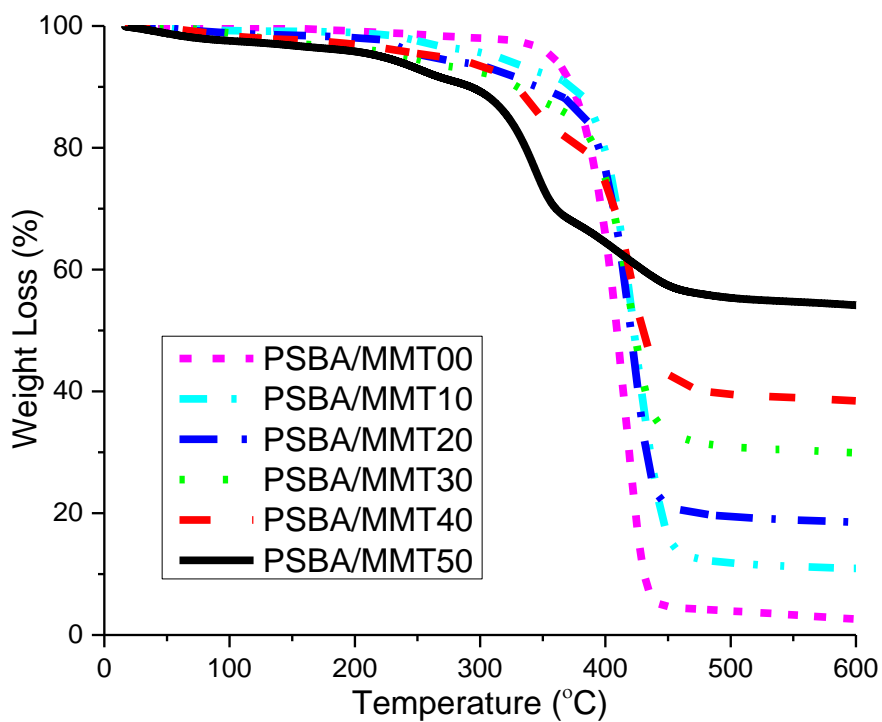*(b) PSBA /MMT20, (c) PSBA /MMT30, (d) PSBA /MMT40, (e) PSBA /MMT50.*

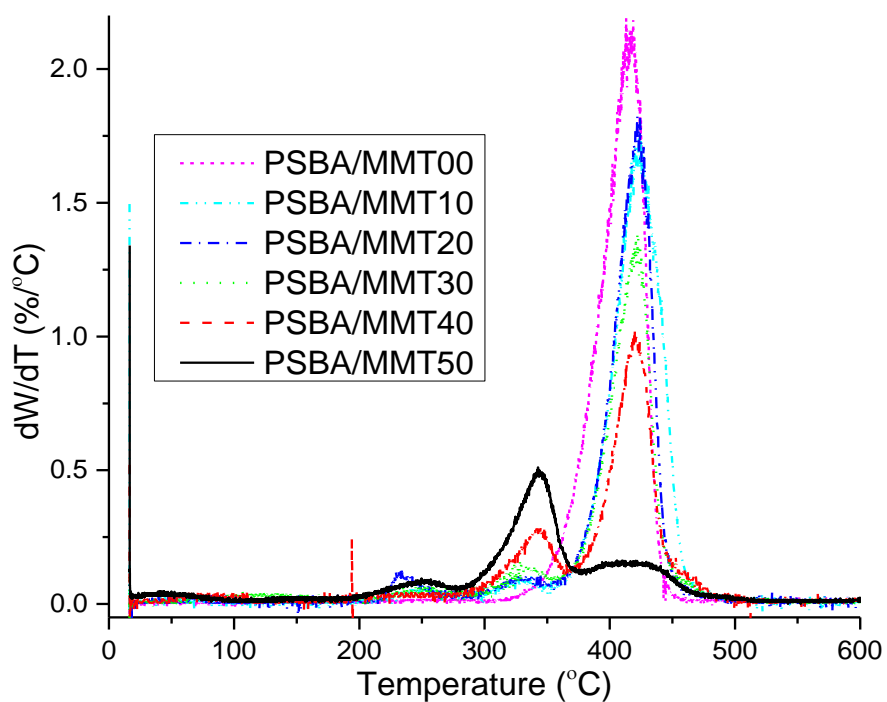*Figure 4.6*: *Thermogravimetric profiles of neat PSBA and PSBA/MMT nanocomposite films*

Figure 4.7: *DTG curves of neat PSBA and PSBA/MMT nanocomposite films*

Table 4.4: TGA data of neat PSBA/MMT and hybrid latexes

Sample	T_{Onset}[a]	m_R[b]
PSBA/MMT00	419.69	2.51
PSBA/MMT10	424.02	10.91
PSBA/MMT20	424.85	18.45
PSBA/MMT30	424.23	29.79
PSBA/MMT40	423.87	38.29
PSBA/MMT50	350.06	54.00

(a) Onset temperature of decomposition (b) Residual weight at 590 ºC

4.3.2.3   Thermo-mechanical properties:

The glass transition temperature was investigated by DSC and the respective values can be seen in Table 4.4 as well as in the heating profiles in Figure 4.7.

There is no particular trend in comparison to the neat latex of the clay. Although there is a slight increase in T_g with the exception of PSBA/MMT50. This is due to the interaction of the filler and polymer matrix that are responsible for the shift in T_g[20]. The behaviour of the nanocomposite latexes corresponds to literature reports where an increase in T_g is observed with respect to the neat latex. This is due to segmental motions of the polymer chains being limited due to the interaction with the clay platelets[13]. The decrease in T_g for PSBA/MMT50 has been explained by percolation threshold which results in the free volume accessible to molecular motions are maximized exhibiting plasticization associated phenomenon[23].

Table 4.5 DSC data of neat PSBA/MMT and PCN films

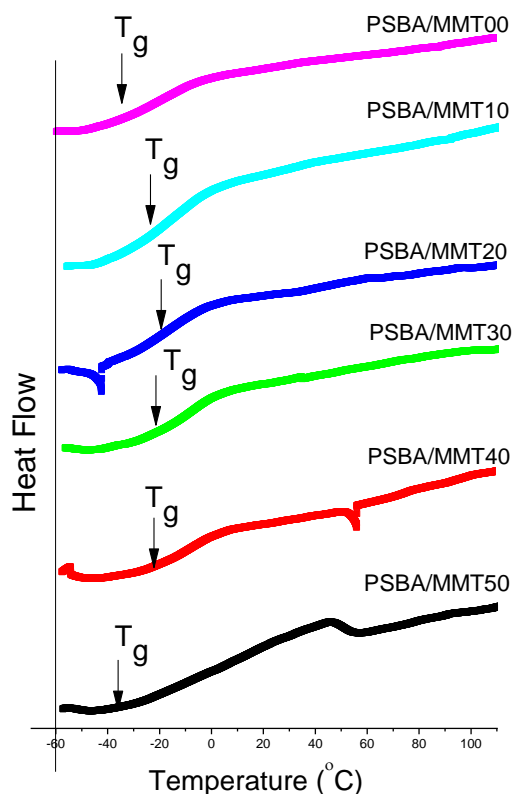| Sample	T_g (ºC)
PSBA/MMT00	-27.51 (theoretical value: 25.4)
PSBA/MMT10	-22.39
PSBA/MMT20	-19.21
PSBA/MMT30	-21.67
PSBA/MMT40	-22.87
PSBA/MMT50	-38.93

Figure 4.8: *Differential scanning calorimetry heating profiles of neat PSBA and PCN films*

The mechanical properties of the materials have been assessed by the following parameters: the storage modulus (Figure 4.8) and damping factor (Figure 4.9).

The samples were prepared as mentioned in Section 3.3.3 and due to the requirement of continuous homogenous films, the nanocomposite latexes were melt pressed. The storage modulus of the scaled up hybrid films, PSBA/MMT00 - PSBA/MMT40, increased as the amount of clay content increased. This behaviour has been observed in literature where Ruggerone[4] produced highly filled nanocomposites using Laponite clay and found an increase in the storage modulus as observed in this study. However conflicting reports suggest that as the clay loading increases the mechanical properties are affected negatively[2,3,14]. The empirical evidence from Section 3.3.2 explains this outcome which is due to the sample preparation (films were melt pressed before DMA analysis). This effect is corroborated by the tan δ peaks in Figure 4.9 which are associated with the T_g and in this case they do not align with the values determined from DSC analysis. While the materials containing up to 40wt.% clay exhibit this increase, the decrease in storage modulus of PSBA/MMT50 with respect to PSBA/MMT40 can be explained by the plasticization effect. This is further evidenced by the decrease in the intensity of the tan δ peak for the corresponding material.

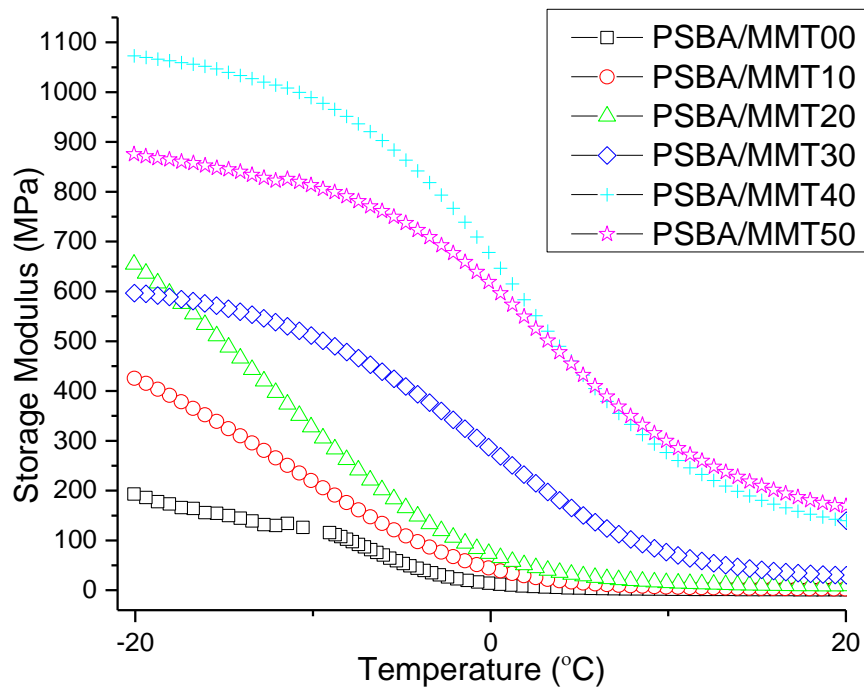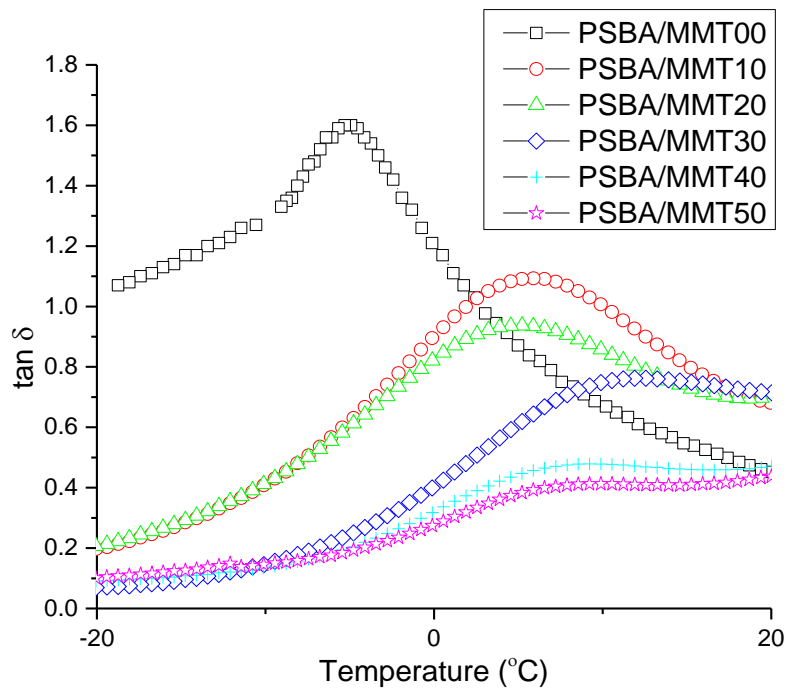*Figure 4.9*: *Storage modulus of neat PSBA and PSBA/MMT nanocomposite films*

Figure 4.10: Tan (δ) peaks of neat PSBA and PSBA/MMT nanocomposite films

4.4   Conclusion:

Polymer clay nanocomposites as well as neat latexes were produced using a scaled up procedure that would be industrially applicable. The use of mechanical shear was

implemented in order to determine if it was a suitable means to replace the use of homogenization devices such as rotor stators or sonicators. The final materials obtained were analysed to establish what effect the structure of the materials has on the properties.

The examination of the effectiveness of the surface modification procedure was found to be fairly successful. FTIR verified the attachment of the characteristic chemical groups and TGA revealed that the efficiency of the ion exchange reaction was inferior to that of previous reports.

The conversion of the nanocomposites were determined gravimetrically and showed minor differences in comparison to the neat latex.

The particle morphology obtained from DLS and TEM for the wet latexes show that there is a large degree of coagulation present especially as the clay content increases including the neat latex which is indicative of instability on the nanoscale. However, to the naked eye the latexes are still homogenous at the time of analysis. The dried latex samples were analysed using micotomed TEM and showed the dispersion of the clay platelets. It is clear that as the amount of clay increases the dispersion decreases and tactoids are seen in samples contains up to 40 wt.% clay

Thermal stability is unaffected by the amount of clay present in the polymer matrix, however, as the clay loading increases, minor degradation takes place which was demonstrated by DTG.

DSC analysis of the materials showed negligible increases in T_g with regard to the neat latex with the exception of PSBA/MMT50 which decreased significantly as a result of the plasticization of the surfactants. Thus the effect of clay loading on the hybrid materials in terms of T_g is minimal up to 40 wt.% clay content.

DMA showed somewhat contradictory behaviour due to the melt pressing of the films where the storage modulus increased as the clay loading increased. This was due to the crosslinking of the films. The damping factor which is related to the T_g did not correspond to the results obtained from DSC. This result further asserts the fact that the films were compromised.

Although the structural features of the hybrid materials on the nanoscale exhibit inferior results the properties seem to either plateau or decrease as the concentration of clay increases up to or including 50 wt.%.

4.5   References

1.   Okada, A.; Usuki, A. *Macromol. Mater. Eng* **2006,** 291, 1449–1476.

2.   Zengeni, E. PhD, Stellenbosch, **2012**.

3.   Zengeni, E., Hartmann, P. C.; Pasch, H. *Compos. Sci. Technol.* **2013**, 84, 31–38.

4.   Ruggerone, R. PhD. Luassane, **2010**.

5.   Mizuno, C.; John, B.; Okamoto, M. *Macromol. Mater. Eng.* **2013**, 298, 400–411.

6.   Belashi, A. PhD, Toledo, **2011**.

7.   Hecht, L. L.; Merkel, T.; Schoth, A.; Wagner, C.; Köhler, K.; Muñoz-Espí, R. Landfester, K.; Schuchmanna, H. P. *Chem. Eng. J.* **2013**, 229, 206–216.

8.   Schork, F. J. U.; Poehlein, G. W.; Wang, S.; Reimers, J.; Rodrigues, J. *Colloids Surfaces A Physiochemical Eng. Asp.* **1999**, 153, 39–45.

9.   Ouzineb, K.; Lordab, C.; Lesauzec, N; Graillata, C.; Tanguy, Philippe A. T.; McKenna, T. *Chem. Eng. Sci.* **2006**, 61, 2994–3000.

10. Anton, N.; Benoit, J.; Saulnier, P. *J. Control. Release* **2008**, **128,** 185–199.

11. Madejova, J. *Vib. Spectrosc.* **2003**, 31, 1–10.

12. Chen, G.; Liu, S.; Chen, S.; Qi, Z. *Macromol. Chem. Phys.* **2001**, 202, 1189–1193.

13. Xue, W.; He, H.; Zhu, J.; Yuan, P. *Spectrochim. Acta Part A* **2007**, 67, 1030–1036.

14. Murima, D. MSc, Stellenbosch, **2015**.

15. Bonnefond, A.; Paulis, M.; Leiza, J. R. *Appl. Clay Sci.* **2011**, 51, 110–116.

16. Asua, J. M. *Prog. Polym. Sci.* **2014**, 39, 1797–1826.

17. Asua, M.; Paulis, M.; Leiza, J. R.; Diaconu, G. *Macromol. Symp.* **2007**, 259, 305–317.

18. Monticelli, O.; Musina, Z.; Russo, S.; Bals, S. *Mater. Lett.* **2007**, 61, 3446–3450.

19. Mishra, A. K.; Allauddin, S.; Narayan, R. *Ceram. Int.* **2012**, 38, 929–934.

20. García-Chávez, K. I.; Hernández-Escobara, C. A.; Flores-Gallardoa, S. G.; Soriano-Corralb, F.; Saucedo-Salazarb, E.; Zaragoza-Contreras, E. A. *Micron* **2013**, 49, 21–27.

21. Voorn, D. J.; Ming, W.; Van Herk, A.M.; Bomans, P.H.H.; Frederick, P.M.; Gasemijt, P.; Johanssmann, D. *Langmuir* **2005**, 21, 6950–6956.

22. Voorn, D. J.; Ming, W.; Van Herk, A. M. *Macromolecules* **2006**, 39, 4654–4656.

23.   Tsai, T.; Lin, M.; Chang, C.; Li, C. *J. Phys. Chem. Solids* **2010**, 71, 590–594.

5 Conclusions and Recommendations for Future Work

5.1 Conclusions

PSBA/MMT materials were produced using a modified miniemulsion procedure referred to as co-sonication. In order to produce stable nanocomposites the clay was compatibilized with the use of a polymerizable surfactant (VBDAC). With the incorporation of up to 50 wt.% clay into the polymer matrix, previous reports using different monomer compositions show different compatibility with the organoclay which can be seen from the resultant properties. The monomer to polymer conversion of the PCNs in comparison to the neat polymer decreased as a function of clay content which was due to the increasing viscosity as the clay content increased. These materials exhibited instability with regard to particle morphology as a result of this increased viscosity. With the analyses of TEM and DLS the particle morphology was found to be unstable as the amount of clay incorporated increased. This was evident by the amount of coagulation and absence of spherical particles present in the TEM images of the hybrid materials compared to the neat latex. Furthermore the dry films exhibited a dispersion of clay platelets which ranged from exfoliated to intercalated as the clay loading increased.

The influence of clay on the properties relative to the neat polymer show increased storage modulus values which were a result of crosslinking of the polymer. The T_g values of the PCN's of up to 40 wt.% increased whereas the loadings of 50 wt.% showed a decrease. This result was due to the restricted molecular motions which is further verified by the decreasing intensity of the tan (δ) peaks associated with T_g. The thermal stability of the PCN's was signified by the change in onset temperature which was seen to decrease as the amount of clay added was increased, additionally the decomposition of the hybrid materials showed a complicated profile leading to the inference that the clay platelets were not homogenously distributed to the point that it affected the weight loss profile.

As a consequence, adequate surface preparation has shown to be crucial because this effects the morphology within the polymer.

The subsequent preparation and characterization of these latexes lead to the next phase in which large volumes of these materials were to be produced which would be industrially relevant.

To save time, cost and increase the organoclay yield the polymerizable surfactant modifier (VBDAC) was replaced with a non-polymerizable one (CTAB). The ion exchange reaction was carried out on a high shear mixer which cut down the processing time for the organoclay. Filtration was used instead of centrifuging. All of the alterations mentioned showed that the procedure is not as efficient as the commonly used method found in literature.

The production of the PCN's showed that certain factors had to be considered such as the method of emulsification. Without the use of sonication, a high energy source and uneconomical route, an alternative means was required. Thus it was proposed that a high speed disperser be implemented in order to form the miniemulsion. This was successful in terms of producing a miniemulsion however the latex morphology showed unstable particles and large amounts of coagulum. The films showed an exfoliated dispersion for loadings of up to 10 wt.% and as the clay loading increased the presence of tactoids become increasingly common. This further verifies the inefficient clay modification. Although the conversion of the hybrid materials hovers around a certain range, it is indicative that the amount of clay does not influence the polymer conversion. The storage modulus indicates stronger nanocomposite latexes however this is a result of the sample preparation where the films were melt pressed causing post cross linking. Where the greatest increase was seen for the sample of 40 wt.% and the sample with the highest loading showed a lower value relative to the strongest latex (that being 40 wt.%). The T_g results showed similar findings to those of PSBA/MMT where the latexes increased in temperature up to 40 wt.% and decreased for loadings of 50 wt.%. The onset temperature showed that the films were unchanged with regard to the neat latex in terms of thermal stability. With the exception of the highest loaded nanocomposite which showed an earlier onset temperature as seen in the DTG graph. Additionally multiple peaks were present which indicates that the film is heterogeneous which correspond the microtomed images showing stacks of platelets.

The comparison of the lab and scaled up procedures showed that the clay modification method in section 4.2 is not as efficient as the standard one in section 3.2 which is evidenced by the thermograms in Figure 4.3 where only 67% of CTAB is attached to the modified clay in comparison to that of 87% (Figure 3.3) using VBDAC in section 3.2. FTIR qualitatively verified this ion exchange reaction for both procedures (Figure 3.2 and Figure 4.2). The morphology of the latex particles which were analysed using TEM (Figure 3.4 and 4.4) as well DLS (Table 3.2

and 4.2) showed that the both procedures produced particles on the order of nanometres. Although the lab procedure showed slightly more stable latexes than the scaled up one. Thermal stability was determined using TGA (Figure 3.6 and 4.6 respectively) and the results obtained were similar for both. The onset temperature of the latexes determined using DTG evidenced this observation. DSC showed the positive influence of clay on the PCNs up to loading of 50wt.% in chapter 3. Where the scaled up PCNs (chapter 4) showed minimal effect in T_g as a result of the clay incorporation with the exception of PSBA/MMT50 sample. The mechanical properties of the materials prepared in chapter 3 and 4 respectively increased as the clay content increased which was a result of post crosslinking. This was further substantiated by the damping factor which is related to the T_g which does not correspond to DSC results. The latex stability of the samples in the scaled up procedure show to be less stable than those produced on lab scale which can be seen in the TEM images as well as DLS. It is also due to the use of a less compatible surfactant used in the scaled up procedure as opposed to the one used in the lab procedure.

In summary the MMT was incorporated into polymer latexes with the material properties of the PCNs being inferior to the neat latexes. Scaling up shows that although the latex morphology is somewhat compromised the properties compared to those produced on the lab scale. The superiority of the lab scale materials are also due to the use of a polymerizable surfactant used in the surface modification procedure. Where a non polymerizable surfactant was used in the scaled up procedure which decreased the compatibility the clay and monomer.

5.2   Recommendations for future work

The scaling up procedure is of interest since miniemulsions are not utilized commercially due to the challenges such as homogenisation equipment alternatives due to the high viscosity of the hybrid miniemulsions with regard to highly filled PCNs. Further work on these dispersions in order to optimize the conditions to produce stable particles would be of significance.

Investigating other polymer matrices that would be more compatible with the clay that are also relevant to coating applications would be of interest. Also extending the study to include other polymerizable surfactants which would promote polymerization as well as increase dispersion efficiency.

Modifying the ion exchange process would also be of assistance in order to produce a better quality organoclay.

Identifying other economically viable resources with regard to clay, such as bentonite, would also be of value.